Machine Learning Informed Microscopy Characterization on Defects

NATIONAL HIGH MAGNETIC FIELD LABORATORY

Sam Mao

Florida A&M University-Florida State University
College of Engineering

Funded by the National Science Foundation (DMR-1644779) and the State of Florida.

U.S. DEPARTMENT OF ENERGY

Zoom Meeting

July12th, 2023

NNSA National Nuclear Security Administration

Support and Acknowledgements

- US Department of Energy (DOE), Office of Science, Basic Energy Sciences
  - ❑ Materials Science and Technology Division
  - ❑ Scientific Users Facilities Division
  - ❑ Including one Early Career Award
- US DOE, Office of Nuclear Energy
  - ❑ Fuel Cycle Research and Development
  - ❑ Nuclear Science User Facilities (NSUF)
  - ❑ Light Water Reactors Sustainability
- US Department Of Defense (DOD)
- US DOE Office of Science, Fusion Energy Sciences
- US National Science Foundation (NSF)

Goal

Upgrade advanced microscopy for materials science characterization from human approach to machine learning approach.

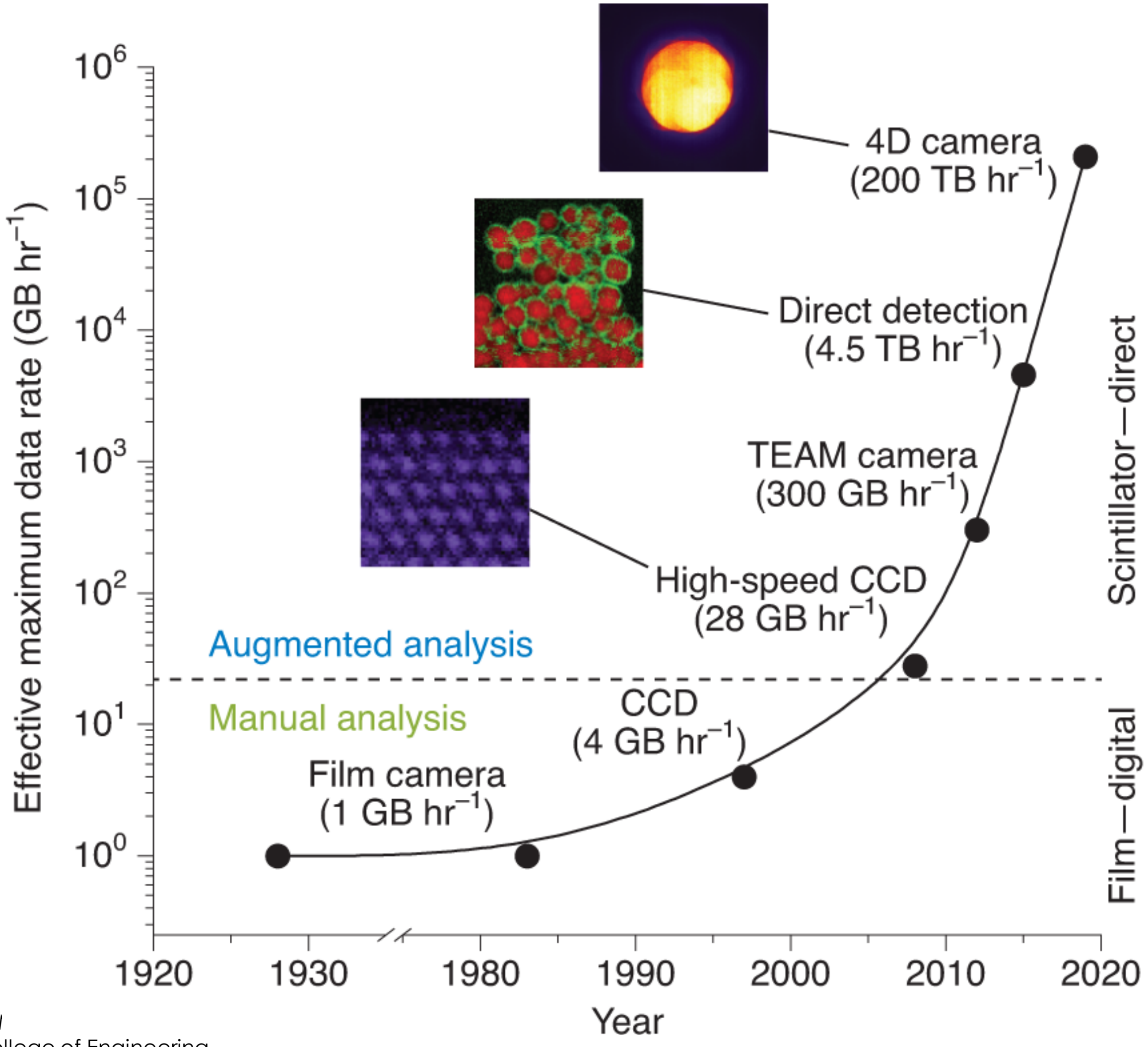

Rapid microscopy data increase!

Spurgeon, S. R., Ophus, C., Jones, L., Petford-Long, A., Kalinin, S. V., Olszta, M. J., ... & Taheri, M. L. (2021). Towards data-driven next-generation transmission electron microscopy. *Nature materials*, *20*(3), 274-279.

Cases

1. **Improve Visibility.**
2. Reveal Chemical Segregation.
3. **Large-scale mapping.**

SCAN ME!

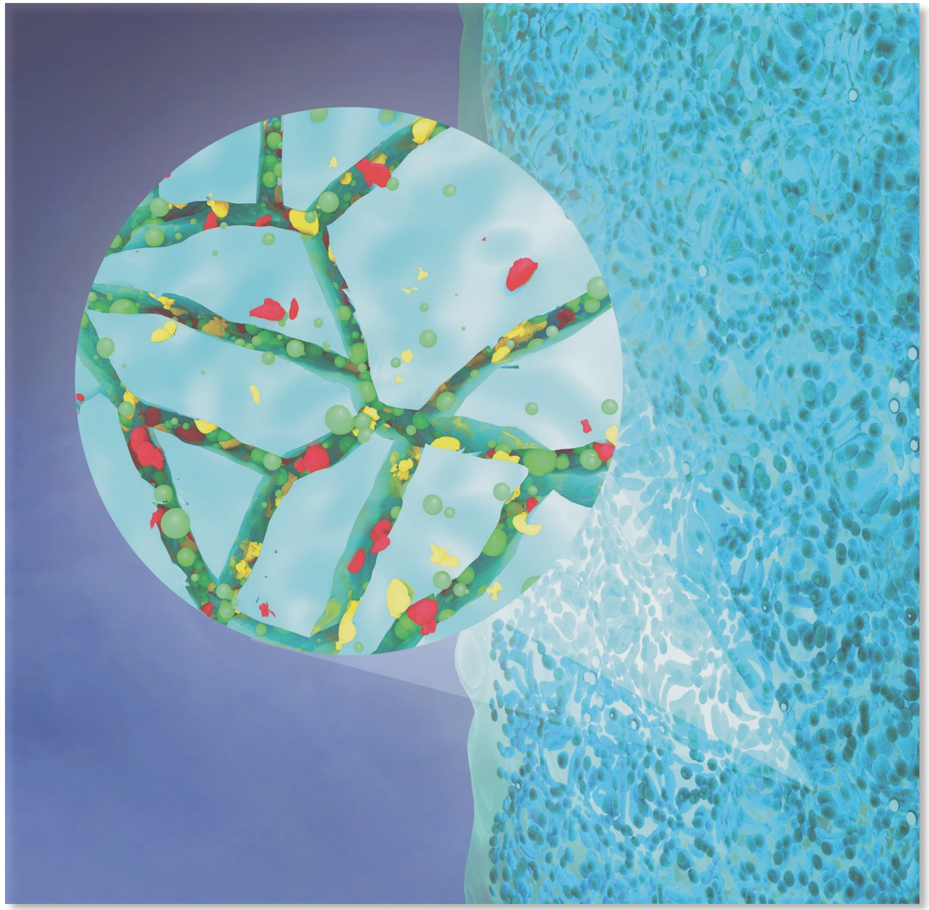

Modern Electron Microscopy for High-burnup Fuels

High-burnup structure (HBS)

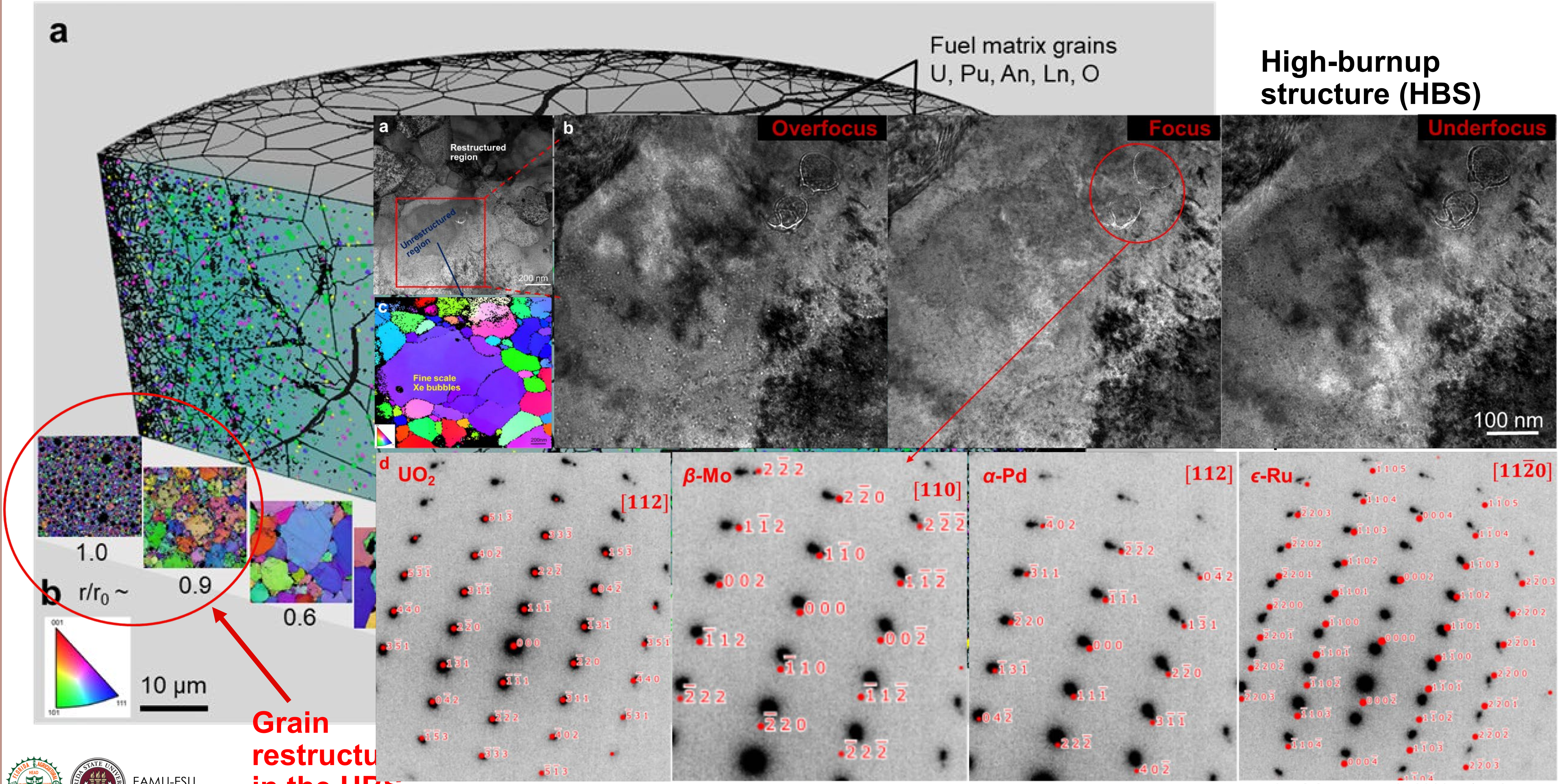

Grain restructuring in the HBS

Machine-learning Enhanced High-throughput X-ray Spectrum Image (XSI) Mapping

$$I(x, y|E) \rightarrow D_{n\times m}$$

$n: x \times y$: total pixels
m: energy channels

each pixel location (*x; y*)

energy bin *E*

photon counting data, the noise is Poissonian.

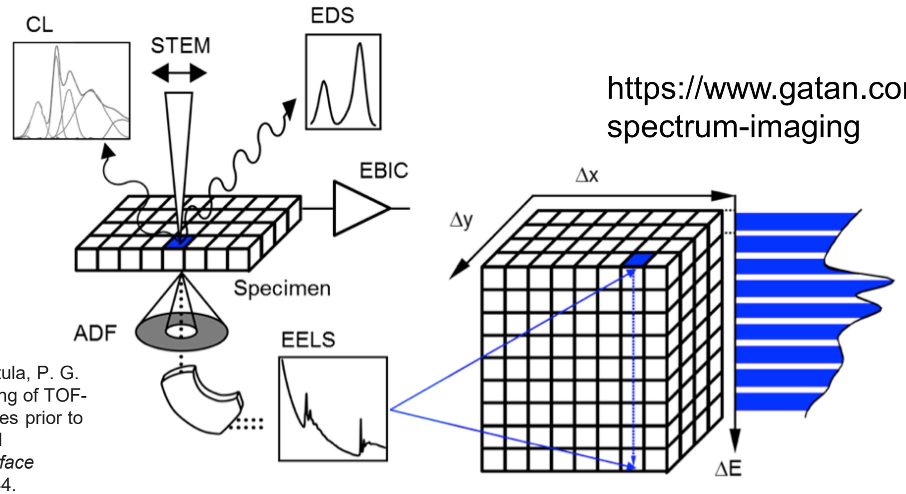

https://www.gatan.com/techniques/spectrum-imaging

Keenan, M. R. (2007). Multivariate analysis of spectral images composed of count data. *Techniques and applications of hyperspectral image analysis*, 89-126.

$$\hat{D} = GDH$$

homoscedastic heteroscedastic

1. Scaling

Stewart, G. W. (1993). On the early history of the singular value decomposition. *SIAM review*, *35*(4), 551-566.

$$\hat{D} = U \sum V^T = \hat{A}\hat{S}^T$$

2. Singular value decomposition (SVD)/ Principal component analysis (PCA)

Keenan, M. R., & Kotula, P. G. (2004). Optimal scaling of TOF-SIMS spectrum-images prior to multivariate statistical analysis. *Applied Surface Science*, *231*, 240-244.

$$D = AS^T = TP^T$$

3. The “fPCA” (factor-PCA) algorithm

$$D = (TR)(R^{-1}P)^T = \tilde{T}\tilde{P}^T$$

4. VARIMAX matrix rotation

Microscopy data acquisition

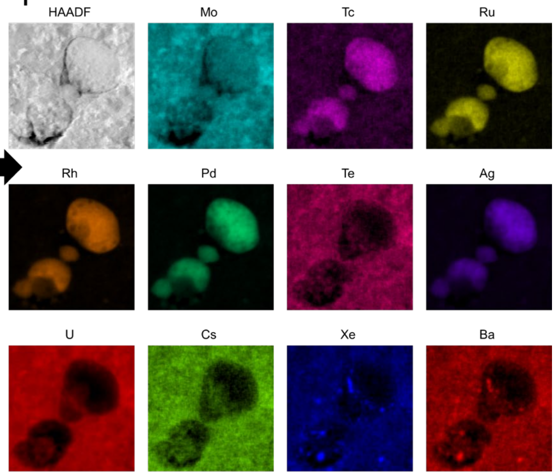

Machine learning module

Original data

4x4 binning

PCA filtering

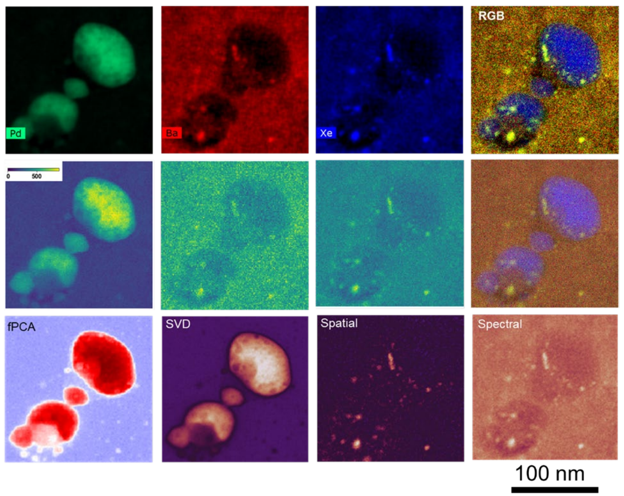

Cloud-based interface for data management

AI-based microscopy data platform

Local Sever

Labelbox Data annotation

aws Online drive

colab Quality control

PySpark ETL & deep learning

Couple with “MAPS” software by Thermo Fisher Scientific

Intragranular Nanoscale Xe bubbles

Spectral simplicity after PCA

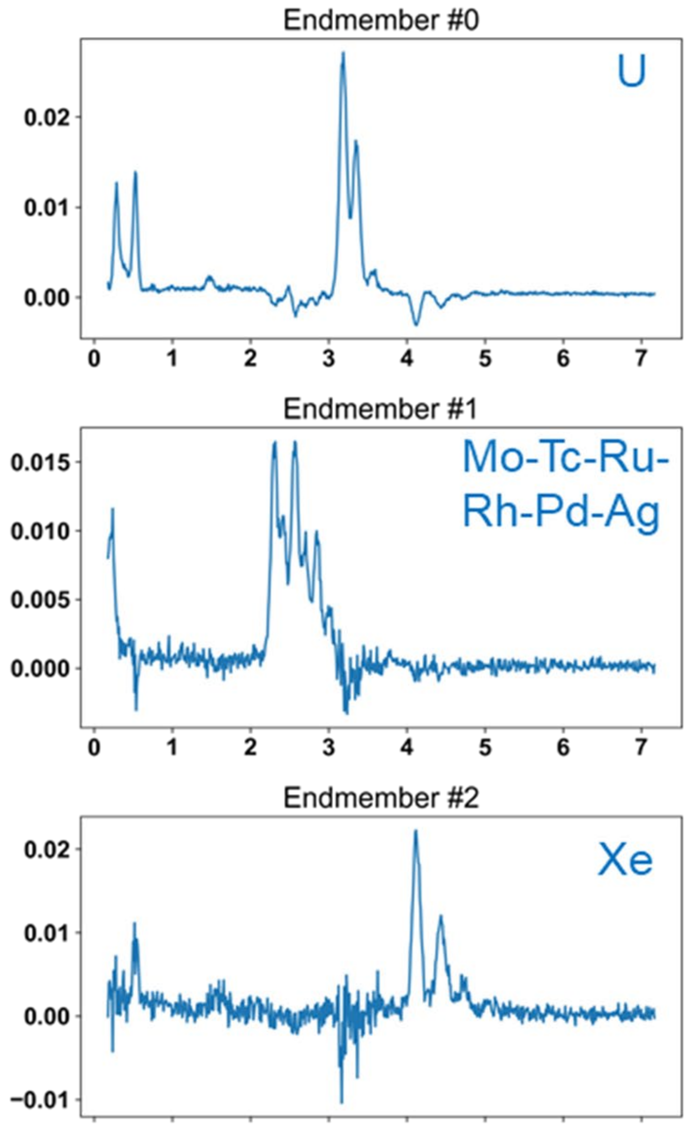

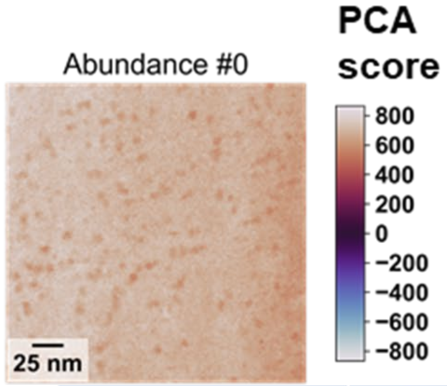

Limerick BWR fuel rod of average burnup at ~56 MWd/kgU (approximately 5-year service in a nuclear power plant reactor).

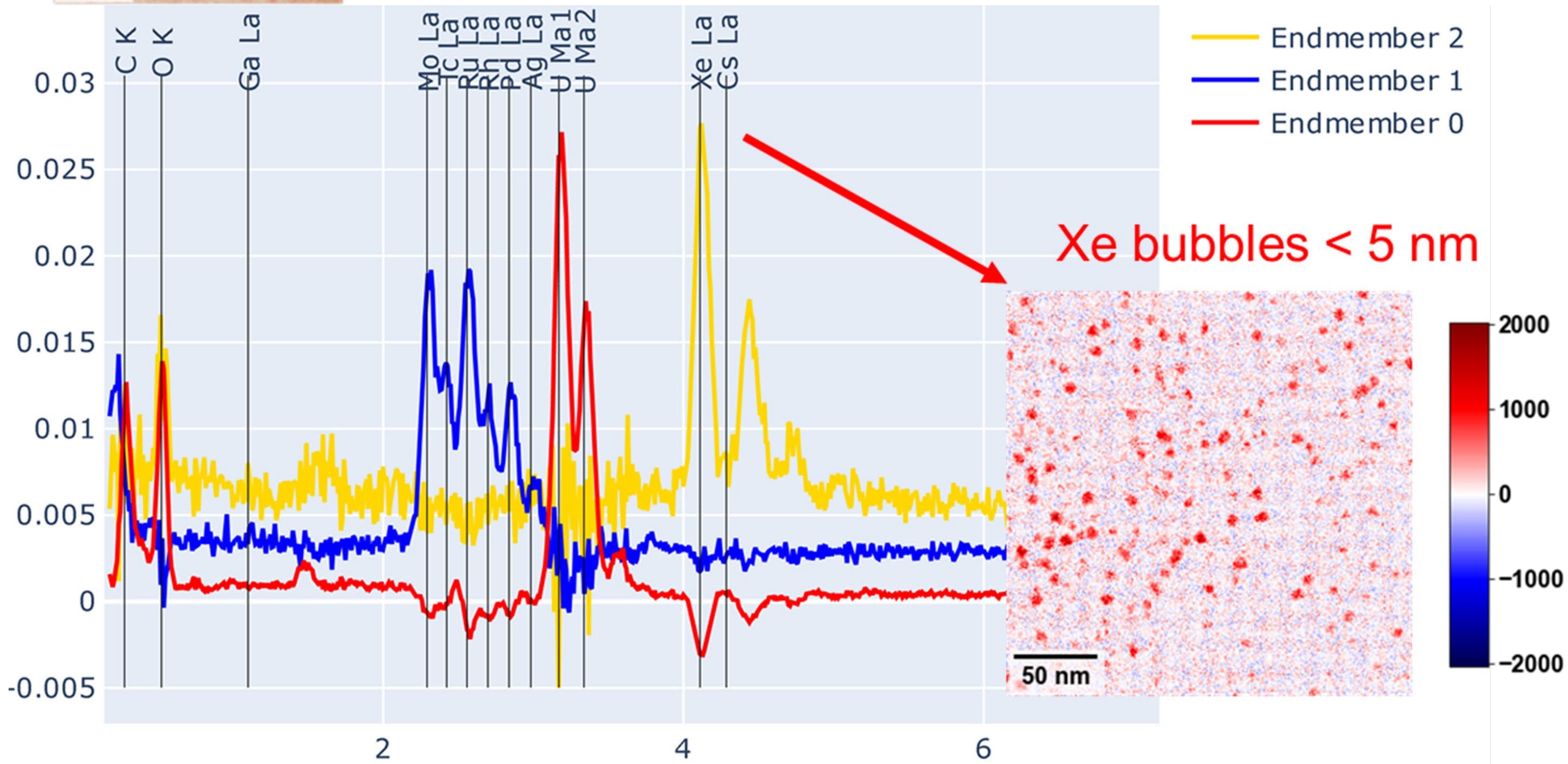

Mao, K. S., Gerczak, T. J., Harp, J. M., McKinney, C. S., Lach, T. G., Karakoc, O., ... & Edmondson, P. D. (2022). Identifying chemically similar multiphase nanoprecipitates in compositionally complex non-equilibrium oxides via machine learning. ***Communications Materials***, 3(1), 1-13.

Unsupervised ML Improves the Visibility of Nanoscale Xe Bubbles at the Grain Boundary

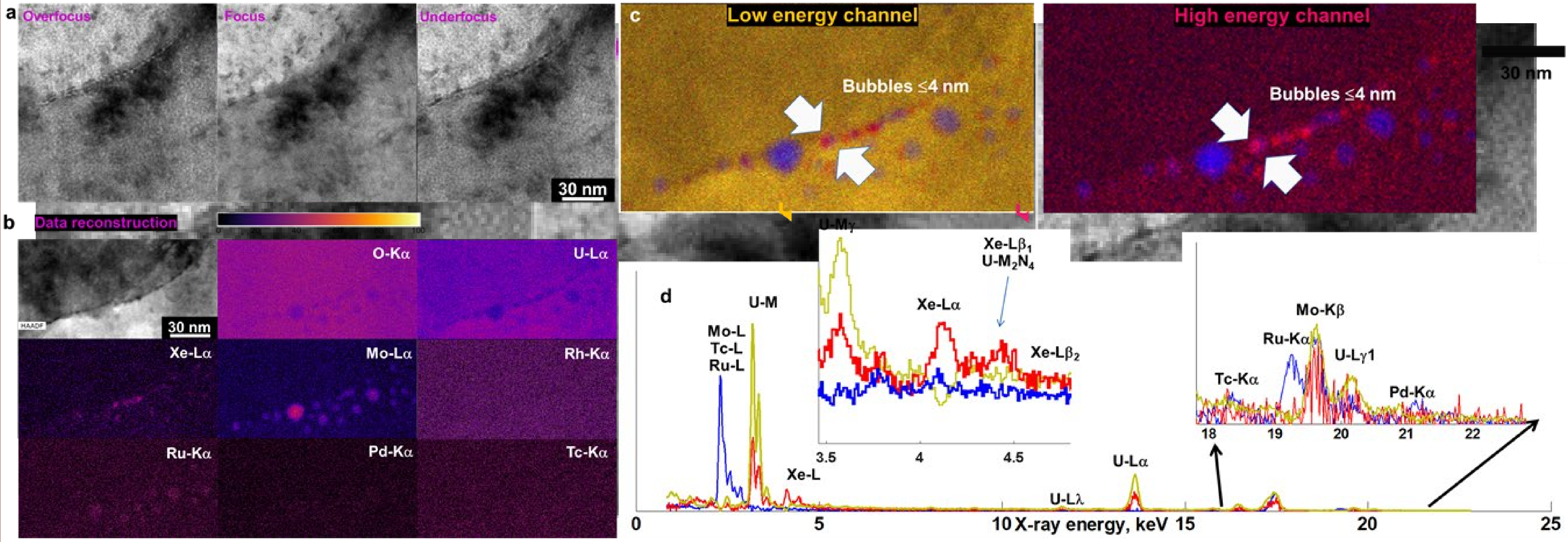

HBS of the H. B. Robinson PWR fuel rod with average burnup at approximately 72 MWd/kgU.

Mao, K. S., Gerczak, T. J., Harp, J. M., McKinney, C. S., Lach, T. G., Karakoc, O., ... & Edmondson, P. D. (2022). Identifying chemically similar multiphase nanoprecipitates in compositionally complex non-equilibrium oxides via machine learning. ***Communications Materials***, 3(1), 1-13.

Materials Informatics–driven Chemistry Analysis on Fission Product Metallic Precipitates along the Radial Position

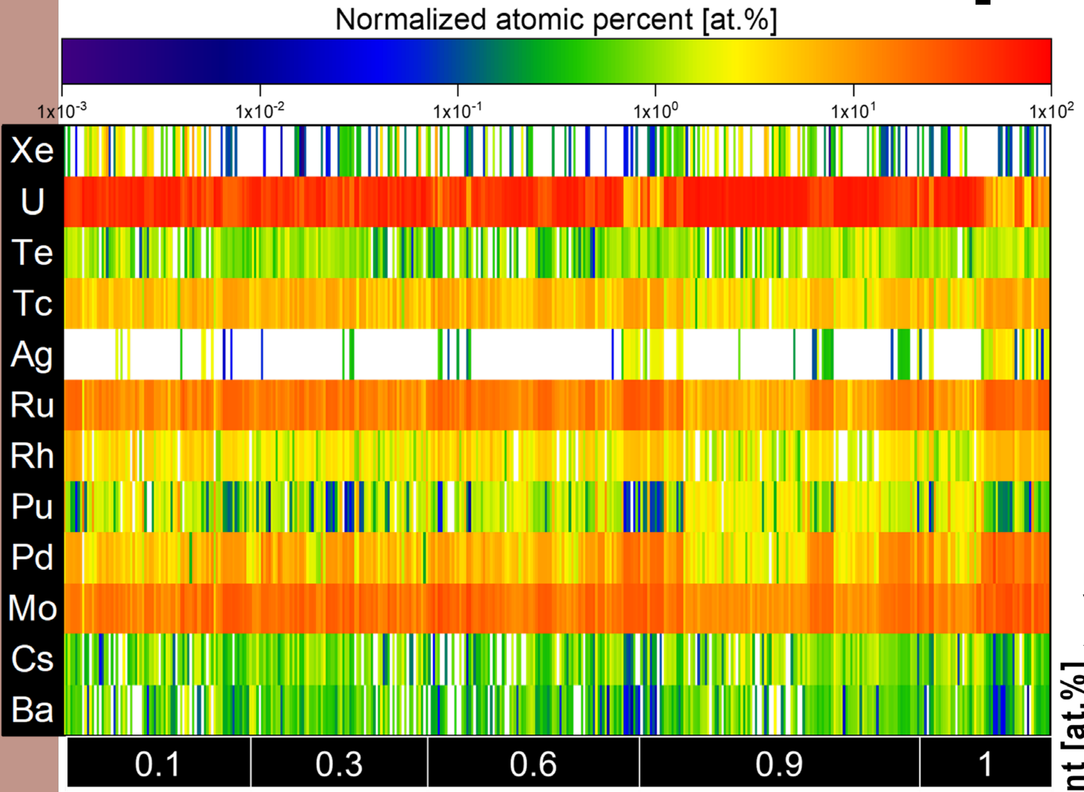

Ternary phase diagram

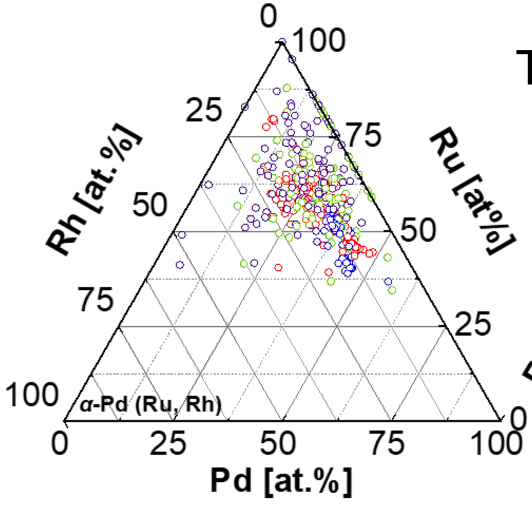

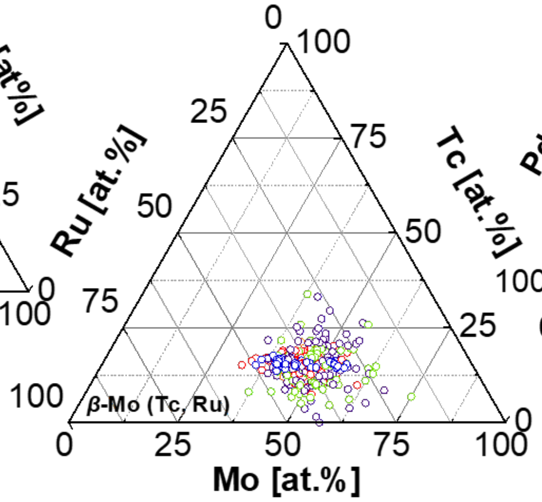

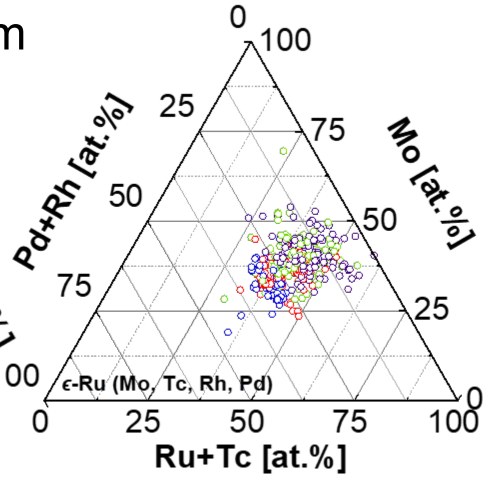

Kleykamp, H., Paschoal, J. O., Pejsa, R. & Thümmler, F. Composition and structure of fission product precipitates in irradiated oxide fuels: Correlation with phase studies in **the Mo-Ru-Rh-Pd** and BaO-UO2-ZrO2-MoO2 Systems. J. Nucl. Mater. 130, 426–433 (1985).

Different with the 80s prediction!

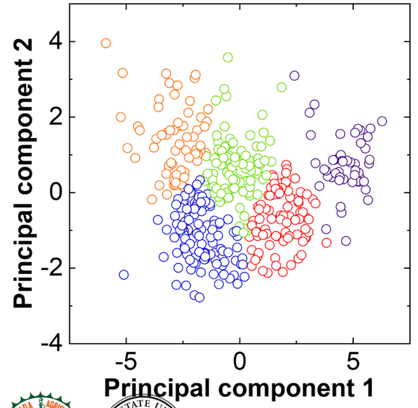

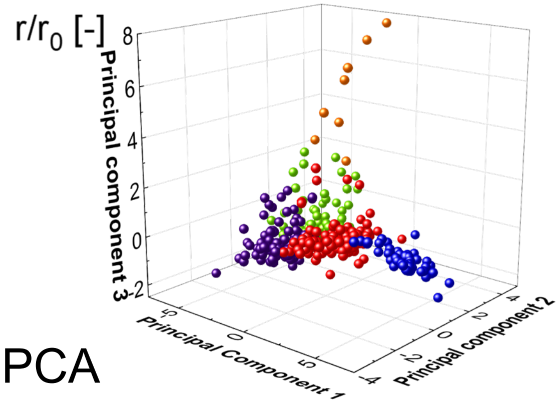

PCA

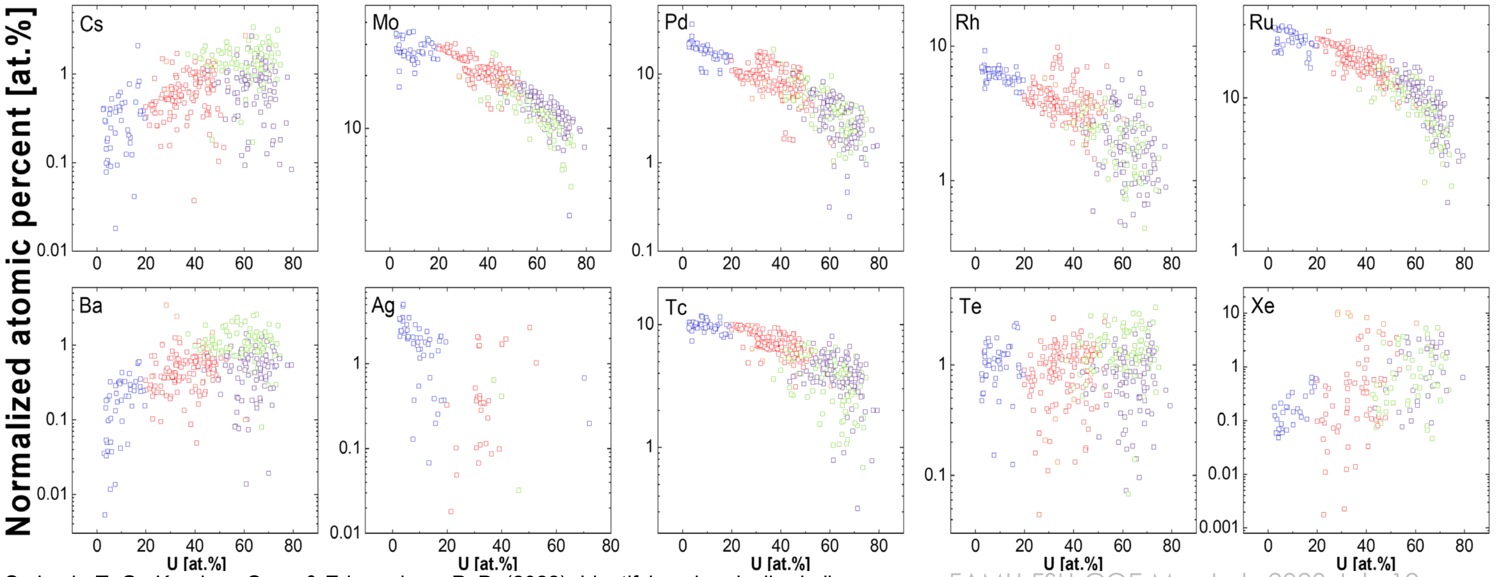

Mao, K. S., Gerczak, T. J., Harp, J. M., McKinney, C. S., Lach, T. G., Karakoc, O., ... & Edmondson, P. D. (2022). Identifying chemically similar multiphase nanoprecipitates in compositionally complex non-equilibrium oxides via machine learning. ***Communications Materials***, 3(1), 1-13.

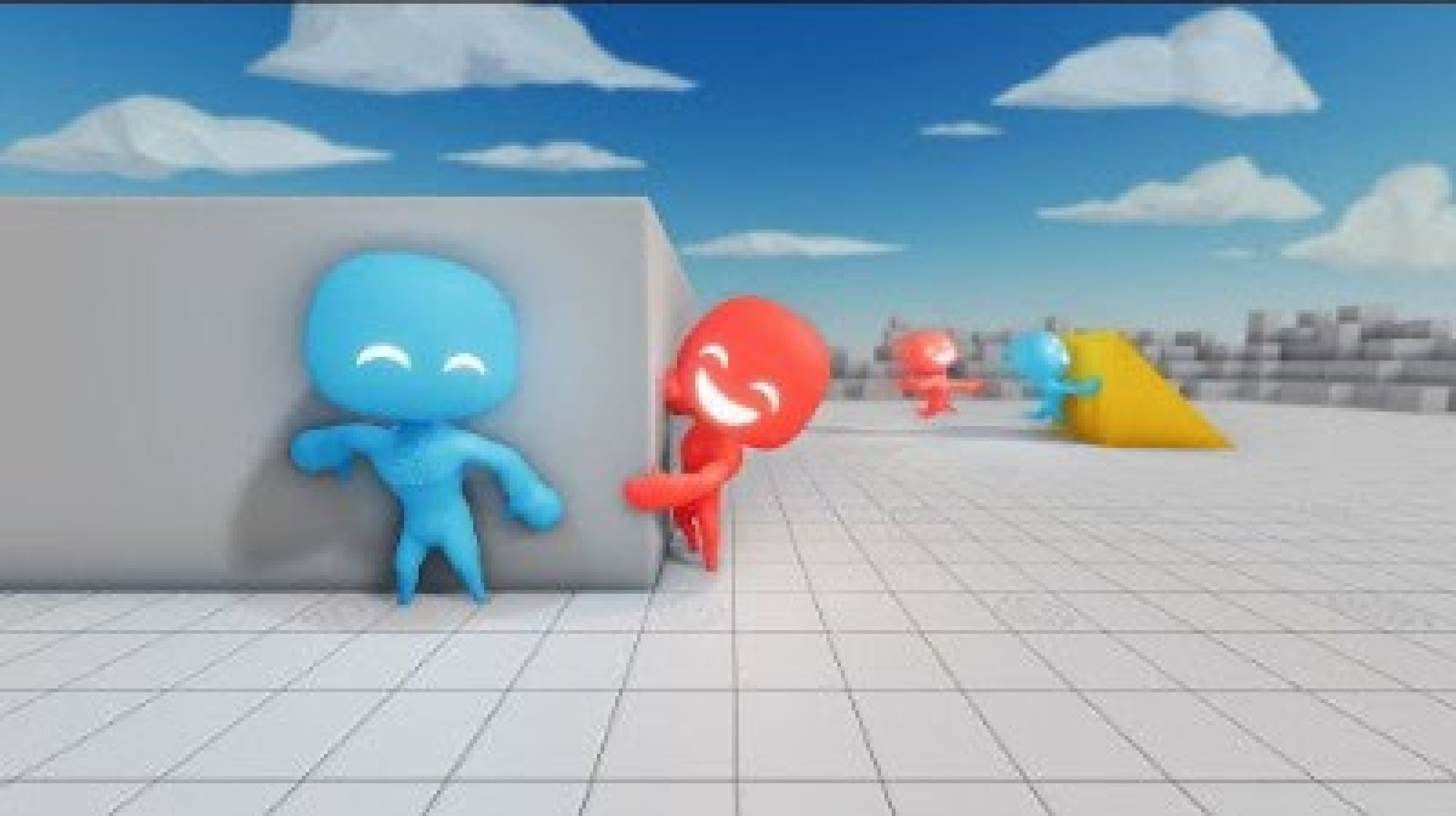

Looking at the Nb_3Sn Grain Boundary (thin film)

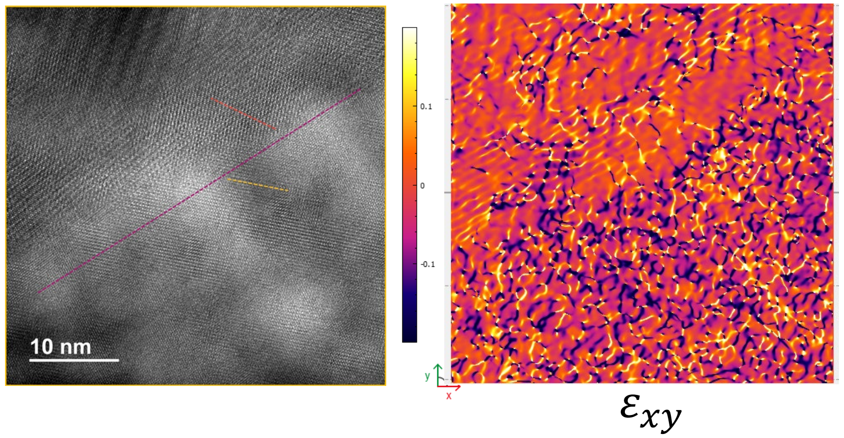

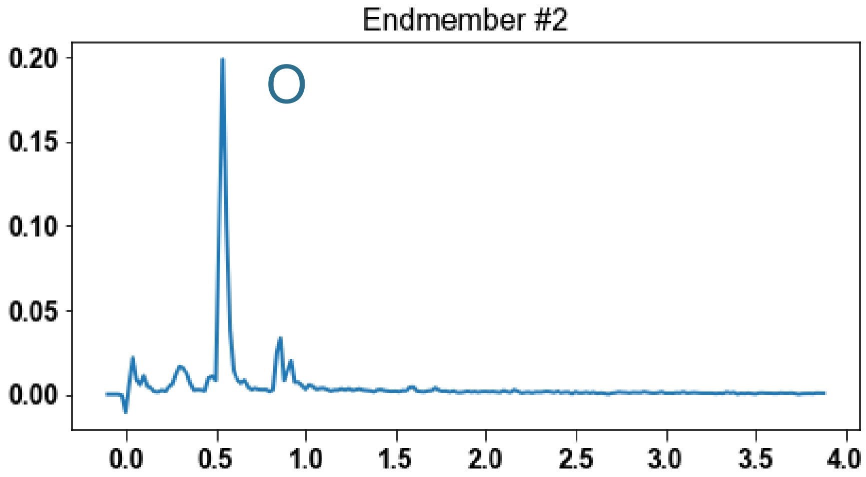

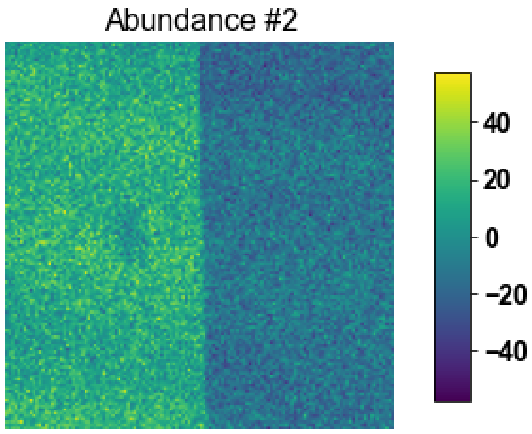

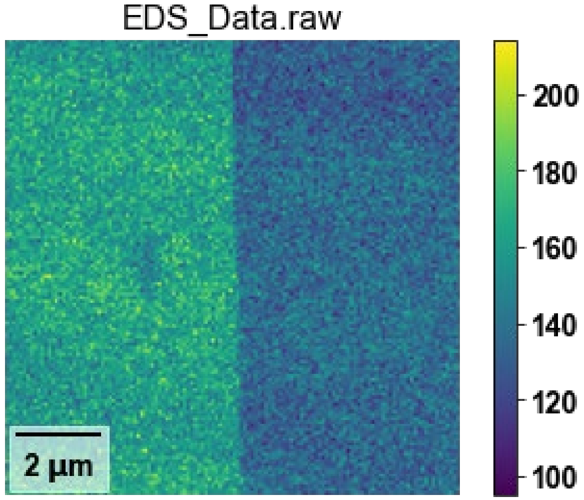

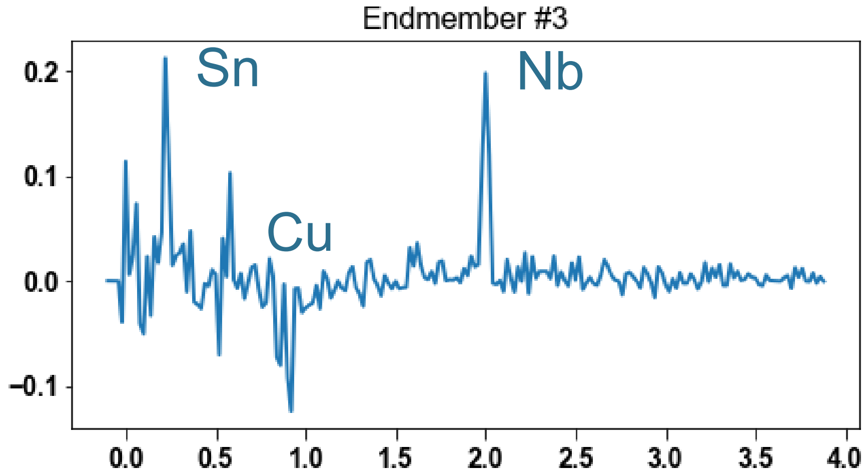

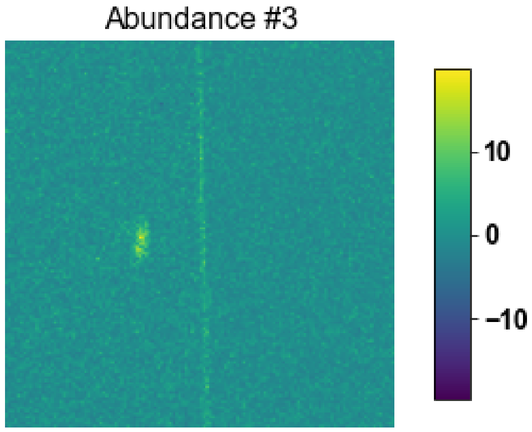

Cu segregation at the GB

Unsupervised Machine Learning STEM-EDS at the GB

Si Map in the Fiber Center using ML Processing

Spectral simplicity after PCA

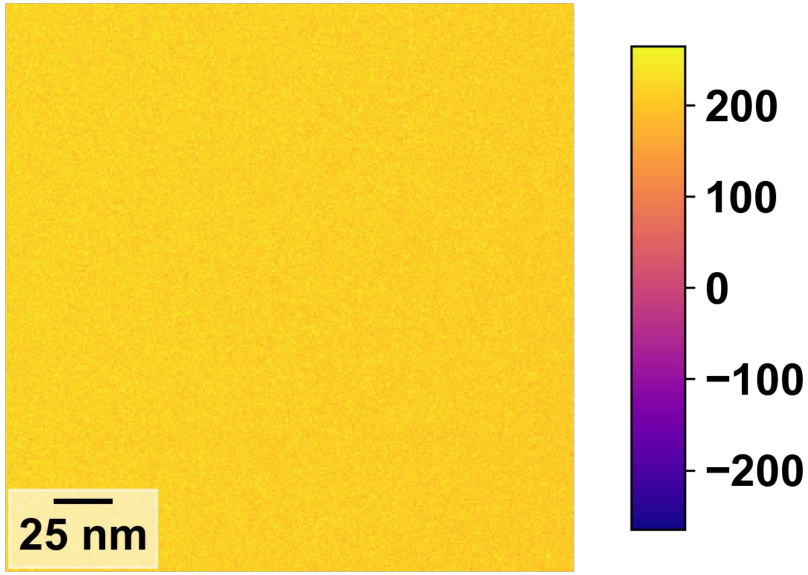

0 dpa

No disordering at low dose
Different Si clusters at higher dpa level!

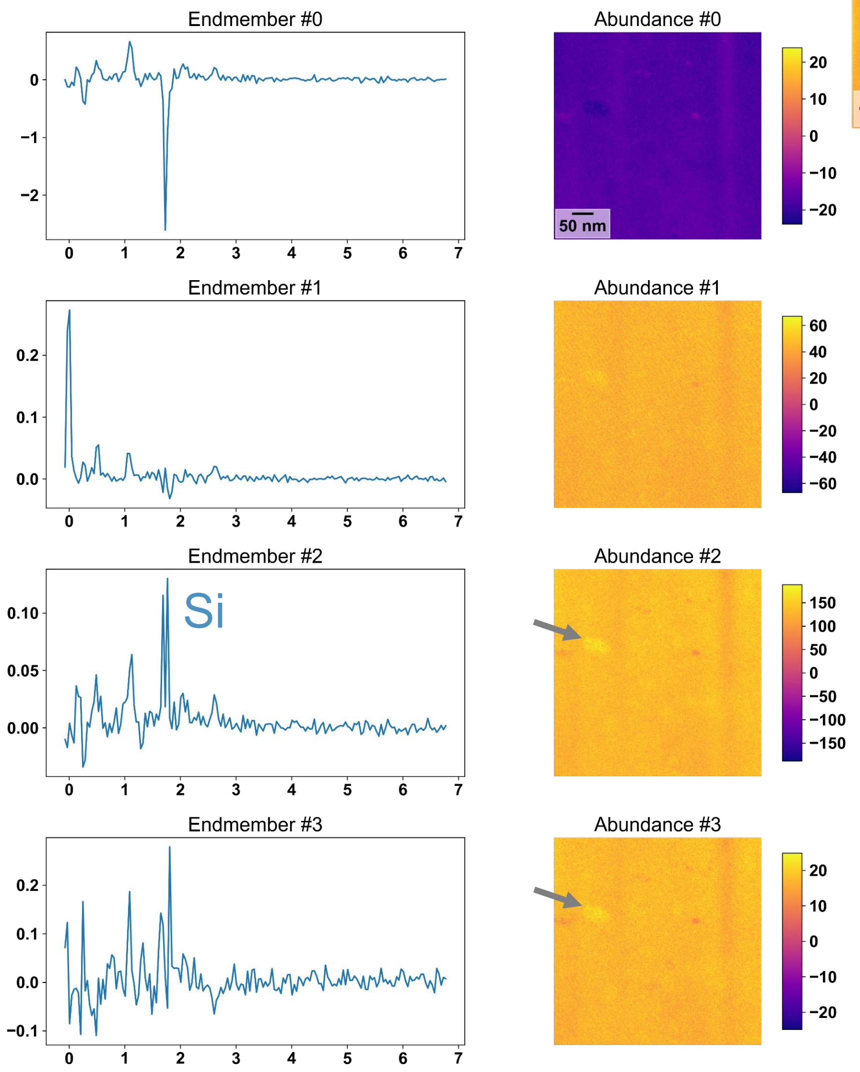

Small Si enriched clusters

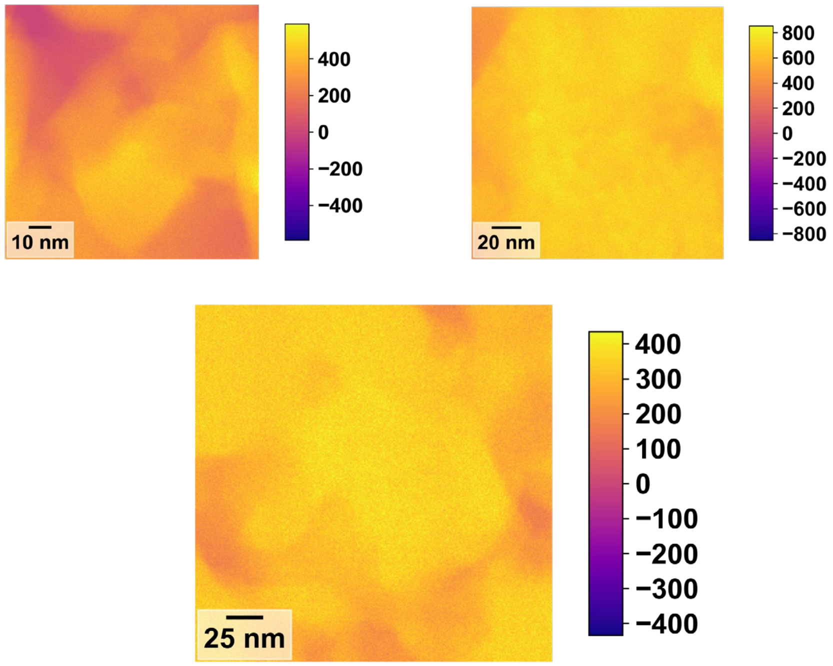

44 dpa

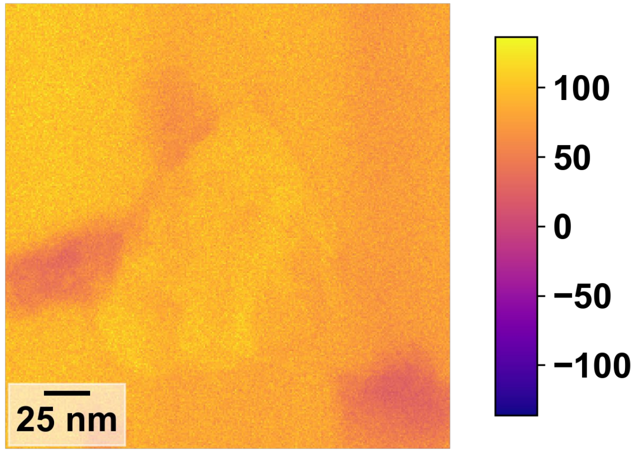

Near fiber edge

Accident-Tolerant High-Strength FeCrAl Alloys with Heterogeneous Structures

Dislocation loops

Improved radiation tolerance with strong sinks

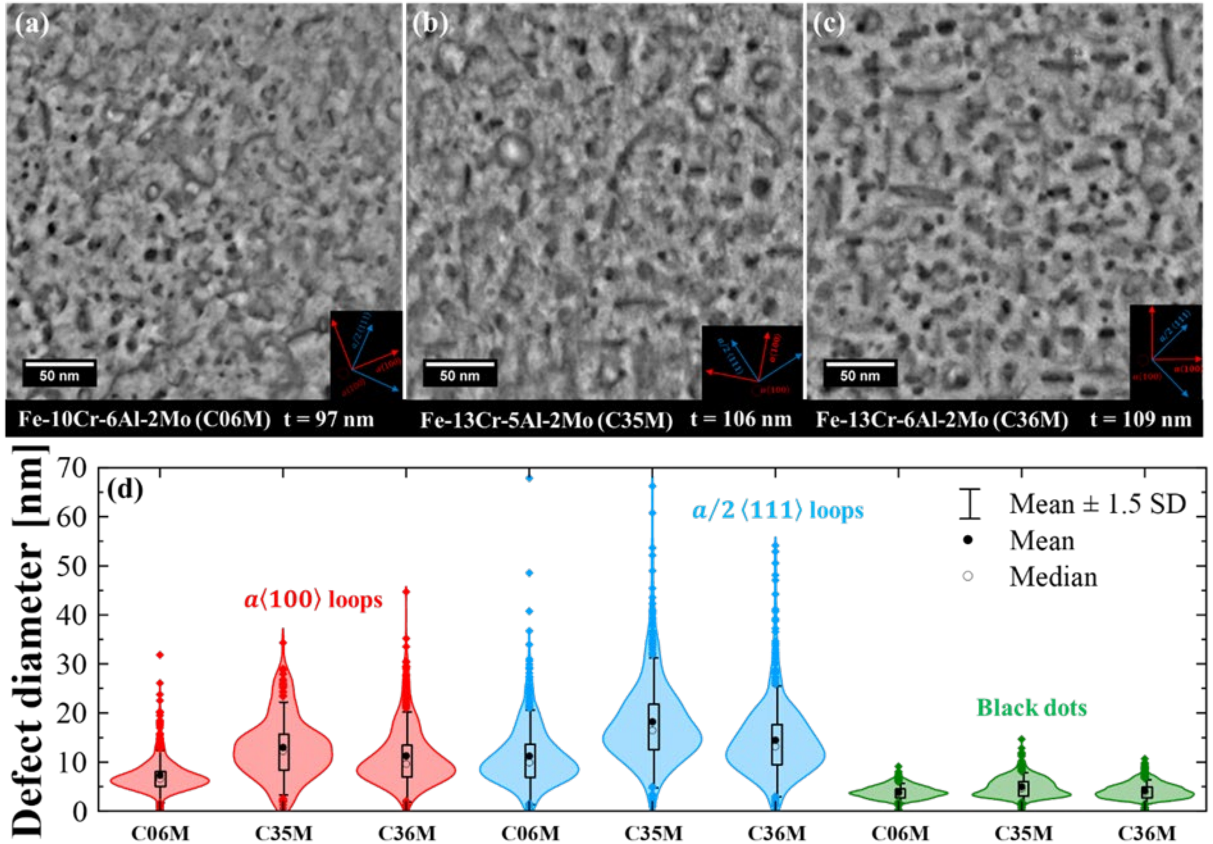

Cr content with heterogeneous structure

7 dpa

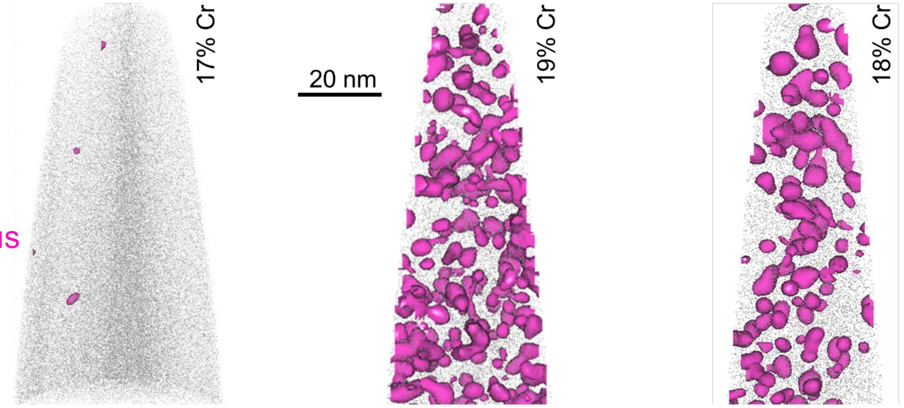

Increasing Cr

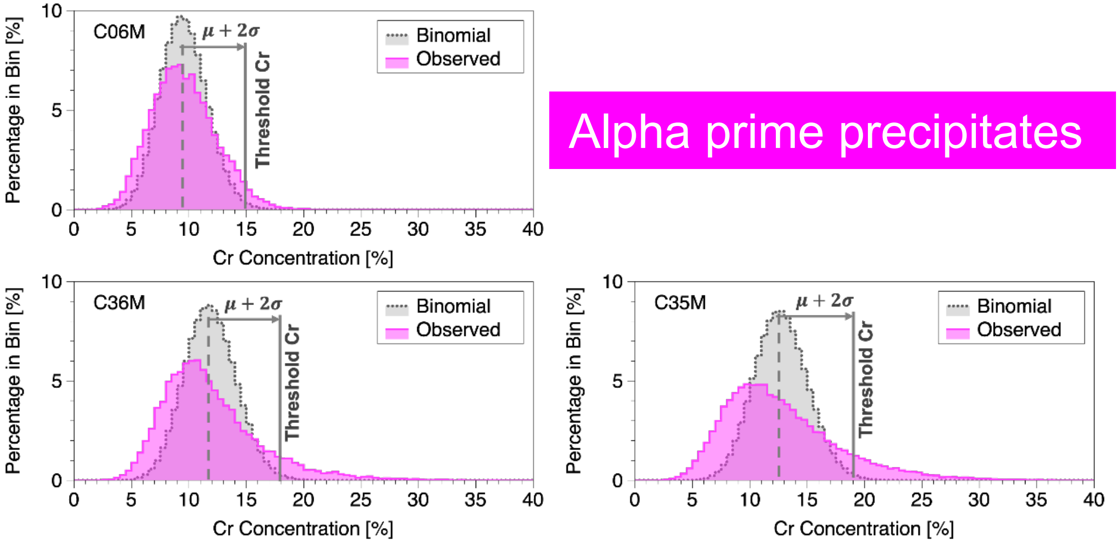

Alpha prime precipitates

Increasing Al

Deep learning module for dislocation loop counting: 500 images within 1 hour.

>> manual counting 10-20 images per hour

Mao, K. S., Massey, C. P., Yamamoto, Y., Unocic, K. A., Gussev, M. N., Zhang, D., ... & Edmondson, P. D. (2022). Improved irradiation resistance of accident-tolerant high-strength FeCrAl alloys with heterogeneous structures. ***Acta Materialia***, *231*, 117843.

Phase Stability & Nanoclustering

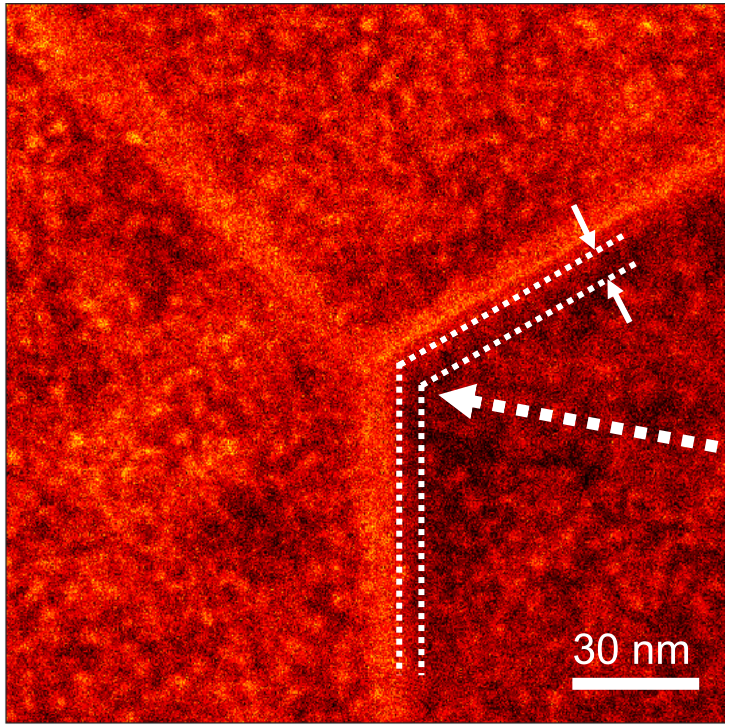

Denuded zone

FeCrAl (Fe-13Cr-5Al-2Mo) C35M alloy neutron irradiated at 7 dpa, 282 °C, 8.16 x 10^{-7} dpa/s

Machine learning (ML) Processing

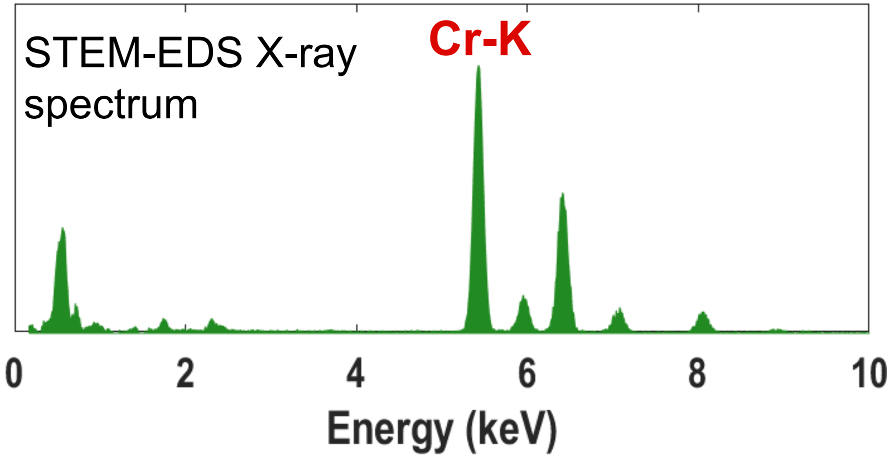

1h map + 10-min analysis

Cr-rich α' precipitates

Denuded zone

Radiation-induced segregation (RIS)

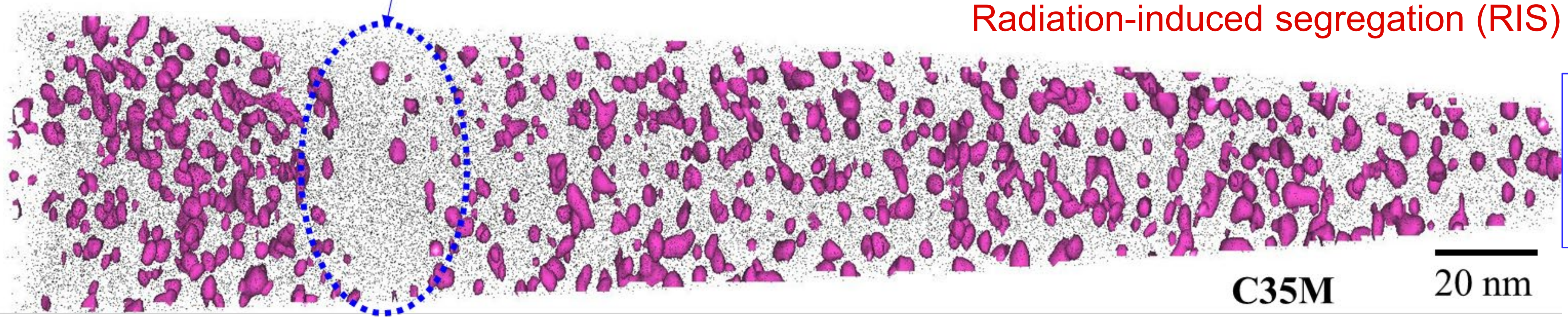

4h data + 4-hr analysis

Grain boundary (GB)

Atom probe tomography-21 at. % Cr isosurface

Chemical Disordering & Amorphization

Fe-Y-O amorphization

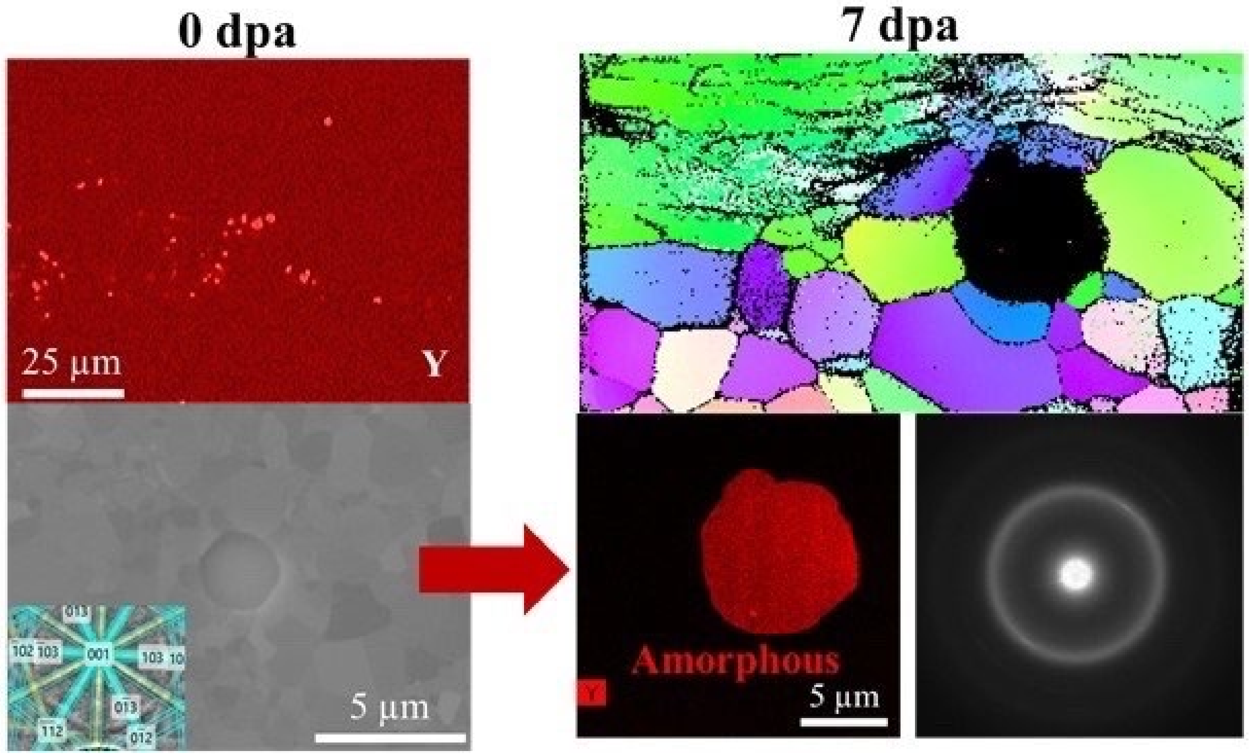

FeCrAl (Fe-13Cr-5Al-2Mo) C35M alloy neutron irradiated at 7 dpa, 282 °C, 8.16 x 10^{-7} dpa/s.

Mao, K. S., Massey, C. P., Gussev, M. N., Yamamoto, Y., Nelson, A. T., Field, K. G., & Edmondson, P. D. (2021). Irradiation-induced amorphization of Fe-Y-based second phase particles in accident-tolerant FeCrAl alloys. ***Materialia***, *15*, 101016.

Representative ML processed map

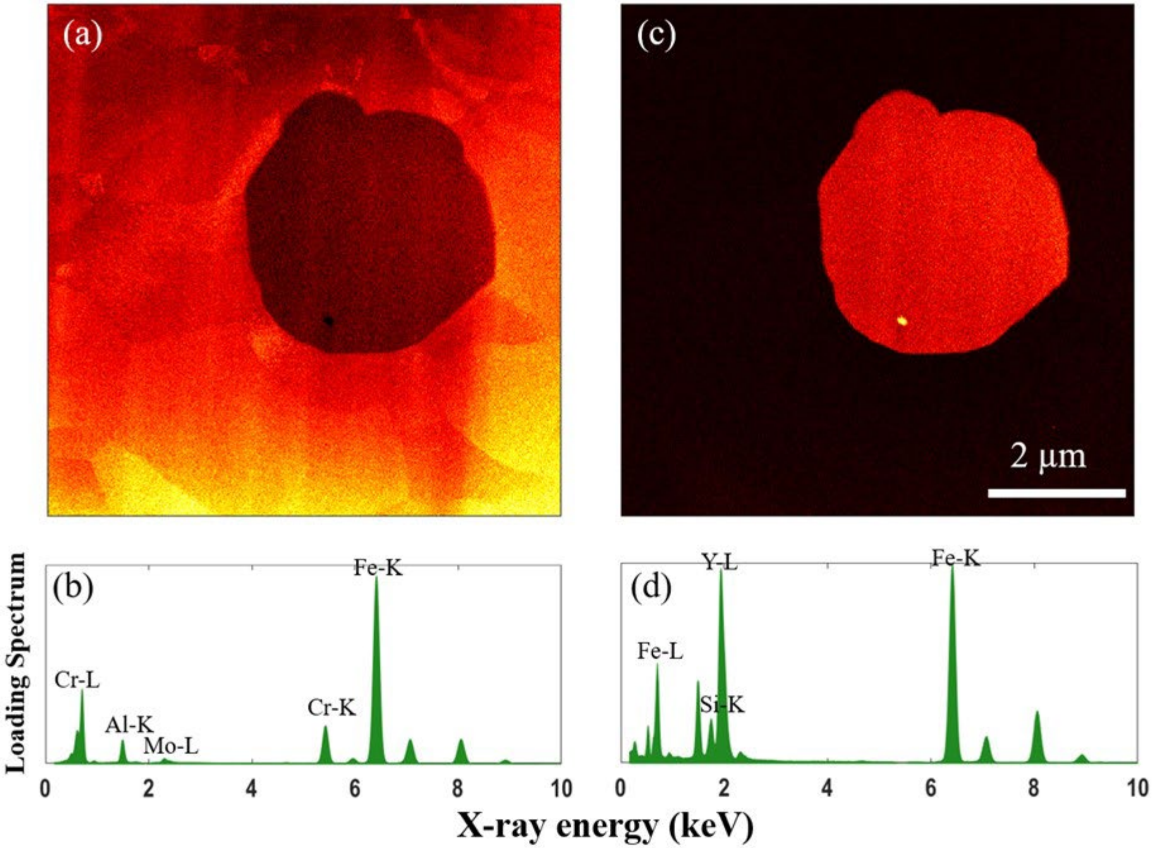

Machine learning increase the confidence of the STEM-EDS map.

Unmatched Irradiation Hardening Model

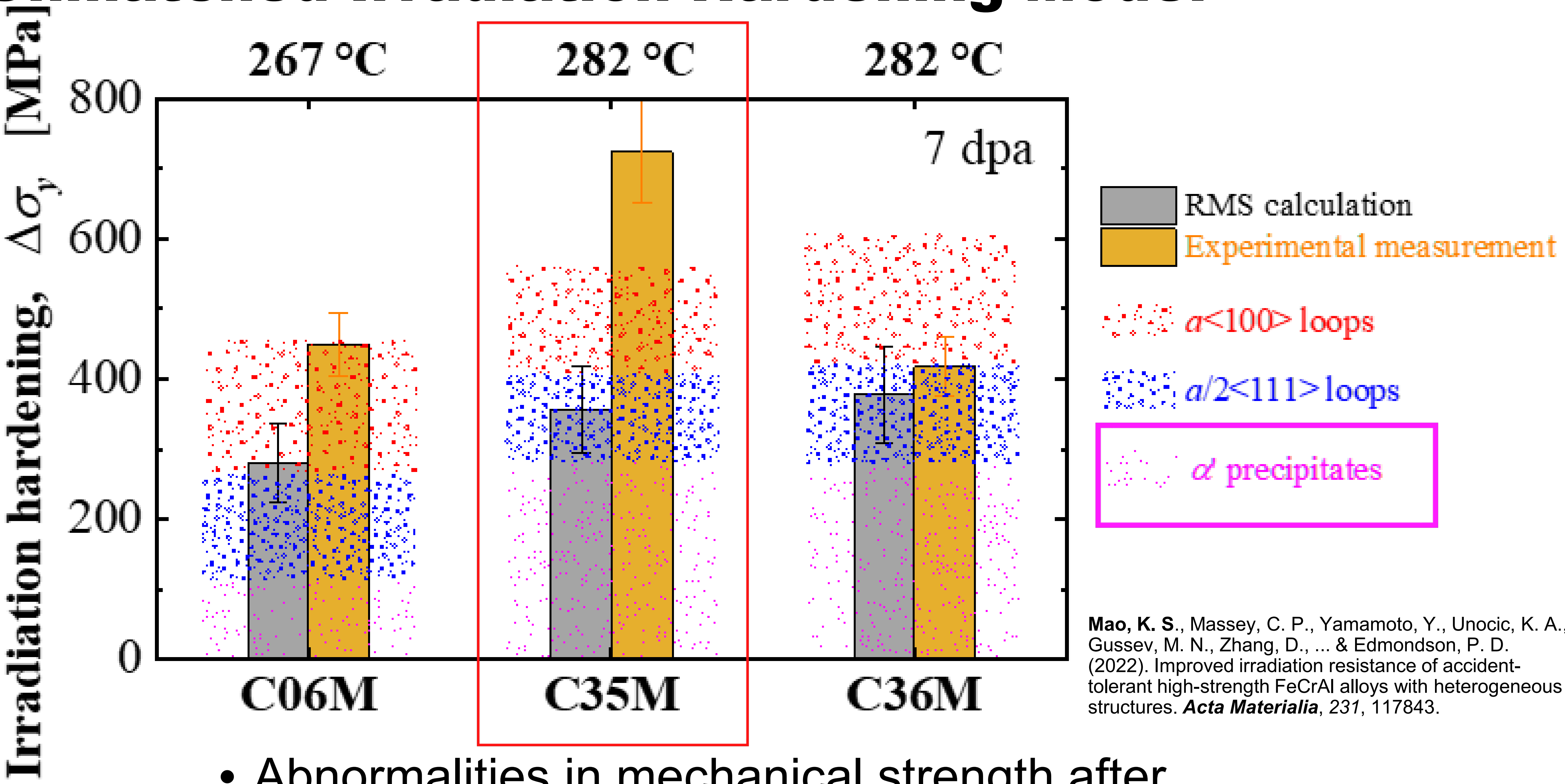

Mao, K. S., Massey, C. P., Yamamoto, Y., Unocic, K. A., Gussev, M. N., Zhang, D., ... & Edmondson, P. D. (2022). Improved irradiation resistance of accident-tolerant high-strength FeCrAl alloys with heterogeneous structures. ***Acta Materialia***, *231*, 117843.

- Abnormalities in mechanical strength after neutron irradiation in C35M.

Unmatched Irradiation Hardening model

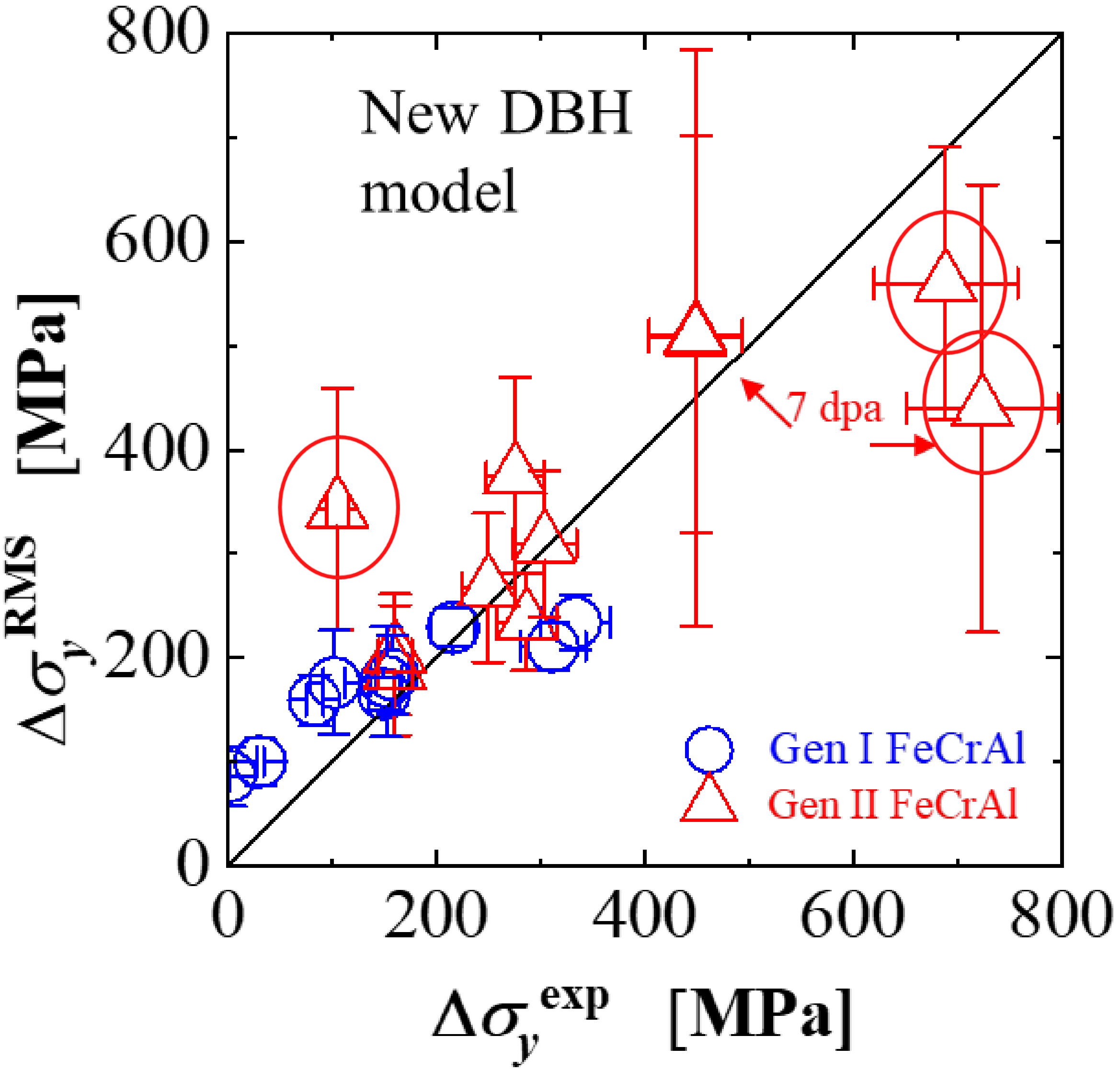

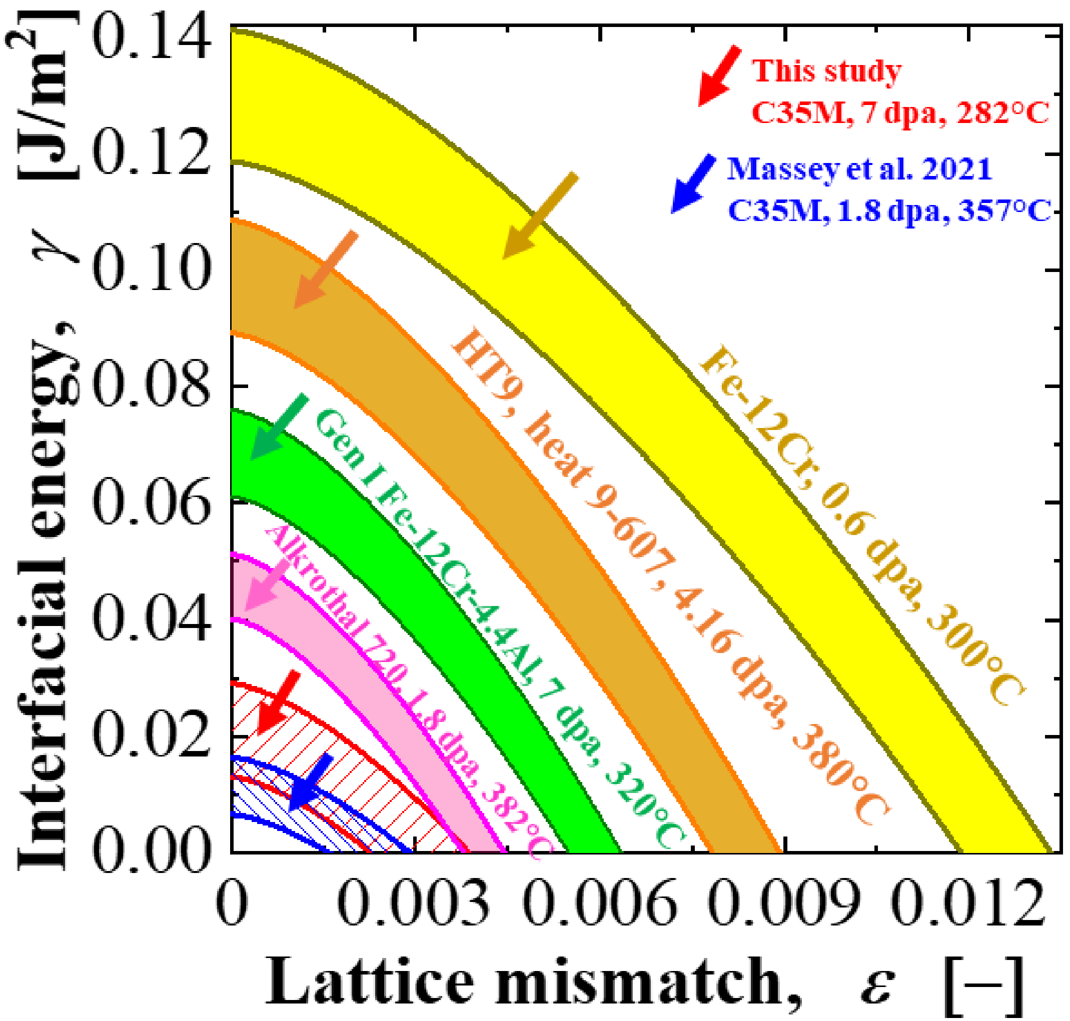

- Destabilize alpha prime precipitation.

Mao, K. S., Massey, C. P., Yamamoto, Y., Unocic, K. A., Gussev, M. N., Zhang, D., ... & Edmondson, P. D. (2022). Improved irradiation resistance of accident-tolerant high-strength FeCrAl alloys with heterogeneous structures. ***Acta Materialia***, *231*, 117843.

Critical Condition for Channel Formation

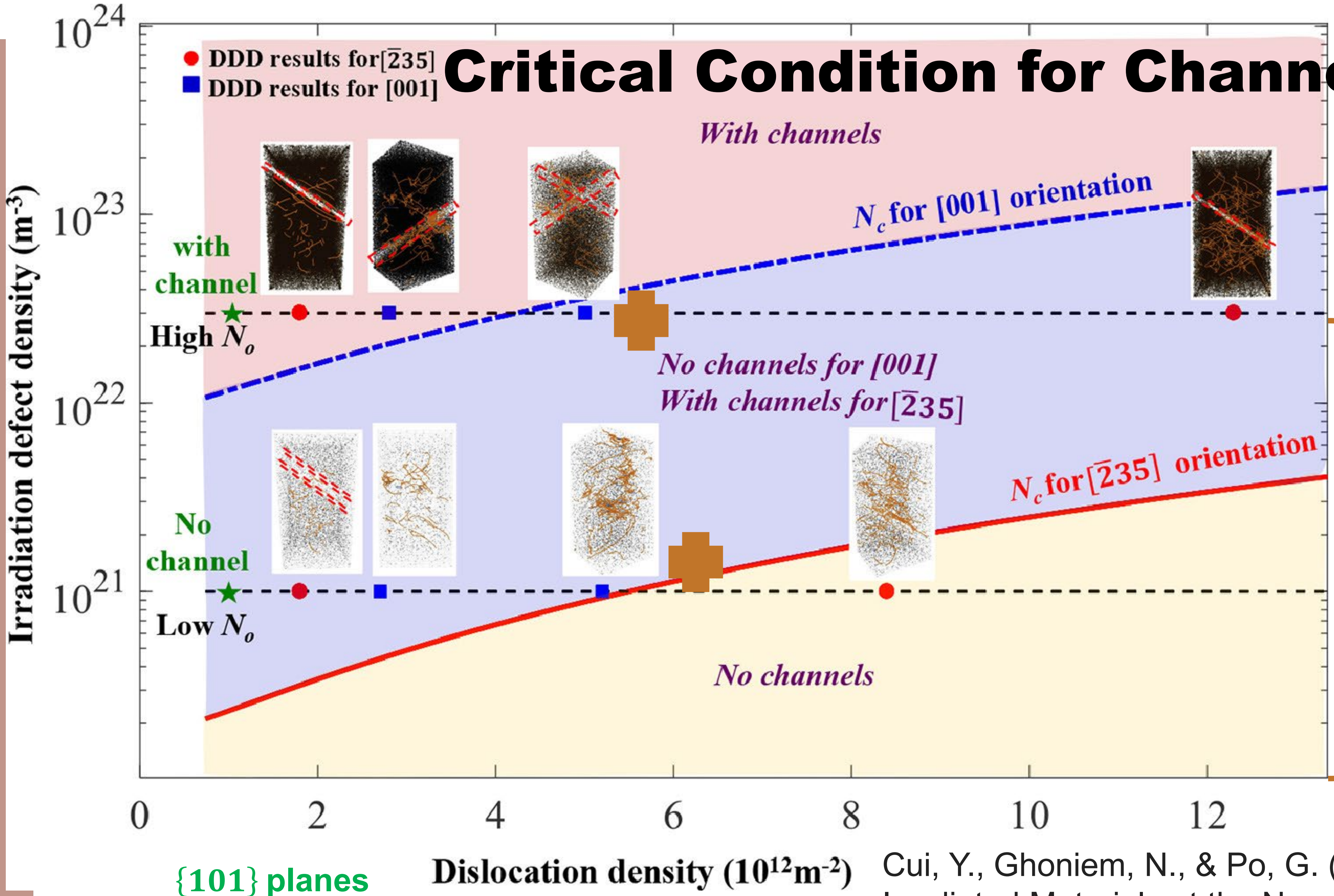

{101} planes

7 dpa, 282 °C

α' precipitates

1.8 dpa, 214 °C

More channels

Loops only

1.8 dpa, 357 °C

Cui, Y., Ghoniem, N., & Po, G. (2020). Plasticity of Irradiated Materials at the Nano & Micro-Scales. *Journal of Nuclear Materials*, 152746.

HRTEM & STEM EELS

ORNL Spallation Neutron Source (SNS) proton-beam window materials-Inconel 718 with increased ductility at 10 dpa with He-related short-range order (SRO) vacancies.

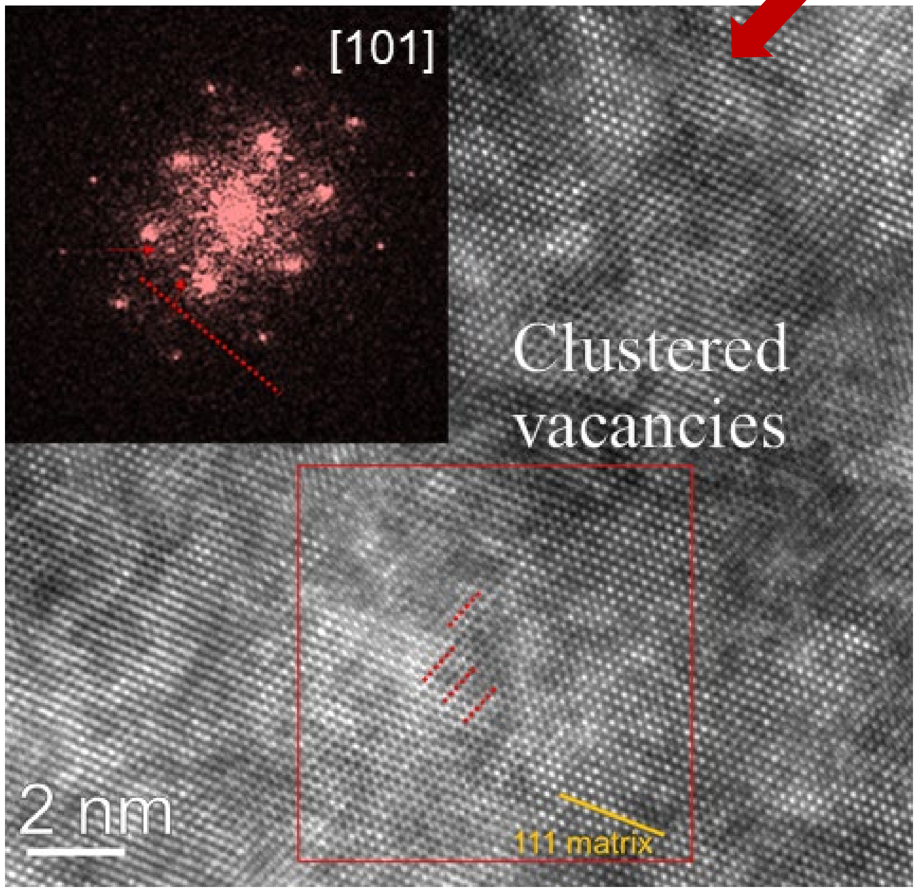

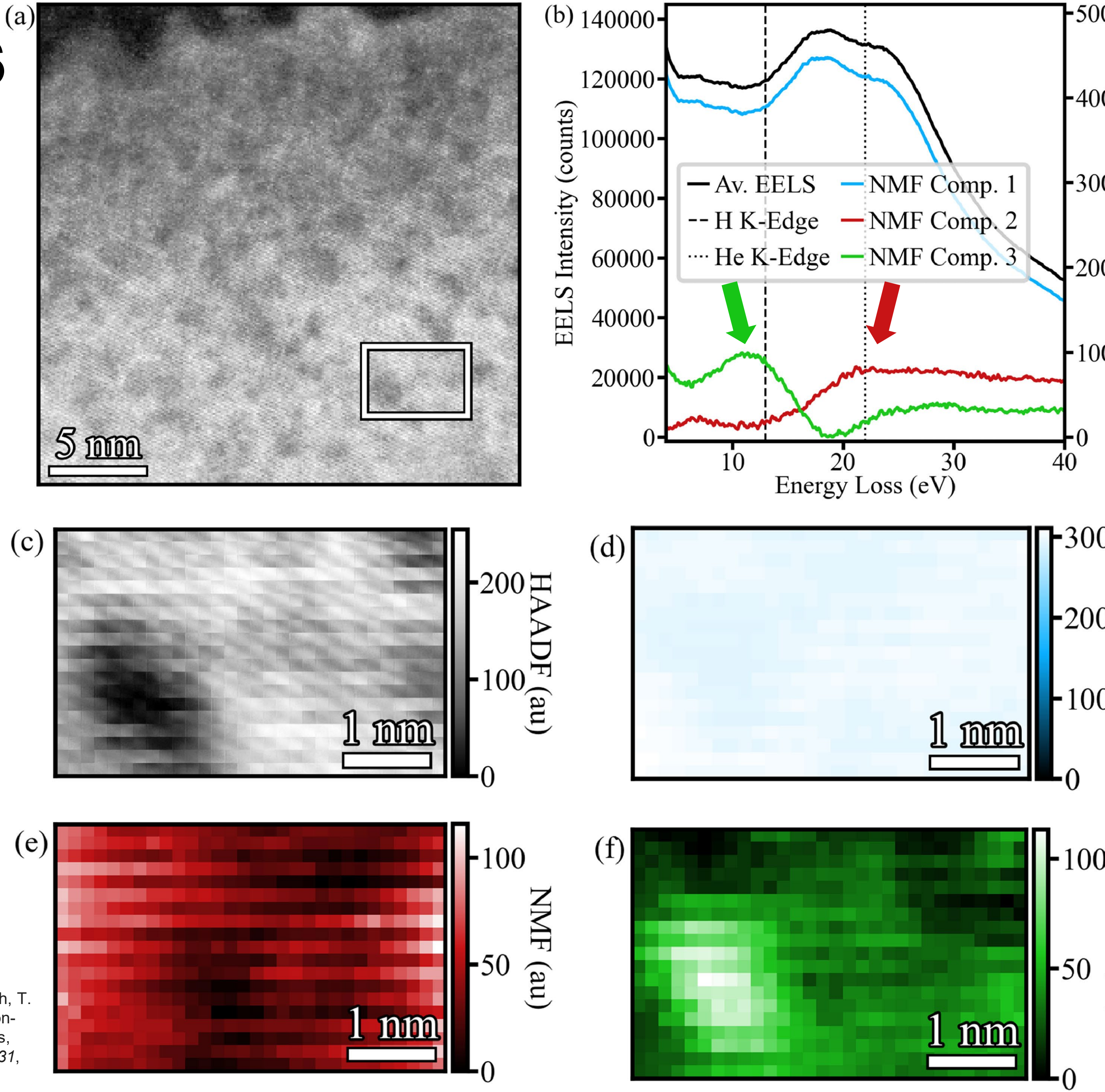

McClintock, D. A., Gussev, M. N., Campbell, C., Mao, K., Lach, T. G., Lu, W., ... & Unocic, K. A. (2022). Observations of radiation-enhanced ductility in irradiated Inconel 718: Tensile properties, deformation behavior, and microstructure. ***Acta Materialia***, *231*, 117889.

NANO LETTERS

ACS AuthorChoice

Letter

pubs.acs.org/NanoLett

Example 1
Live coding

Multicomponent Signal Unmixing from Nanoheterostructures: Overcoming the Traditional Challenges of Nanoscale X-ray Analysis via Machine Learning

David Rossouw,*[†] Pierre Burdet,[†] Francisco de la Peña,[†] Caterina Ducati,[†] Benjamin R. Knappett,[‡] Andrew E. H. Wheatley,[‡] and Paul A. Midgley[†]

[†]Department of Materials Science and Metallurgy, University of Cambridge, 27 Charles Babbage Road, Cambridge CB3 0FS, United Kingdom

[‡]Department of Chemistry, University of Cambridge, Lensfield Road, Cambridge CB2 1EW, United Kingdom

ABSTRACT: The chemical composition of core–shell nanoparticle clusters have been determined through principal component analysis (PCA) and independent component analysis (ICA) of an energy-dispersive X-ray (EDX) spectrum image (SI) acquired in a scanning transmission electron microscope (STEM). The method blindly decomposes the SI into three components, which are found to accurately represent the isolated and unmixed X-ray signals originating from the supporting carbon film, the shell, and the bimetallic core. The composition of the latter is verified by and is in excellent agreement with the separate quantification of bare bimetallic seed nanoparticles.

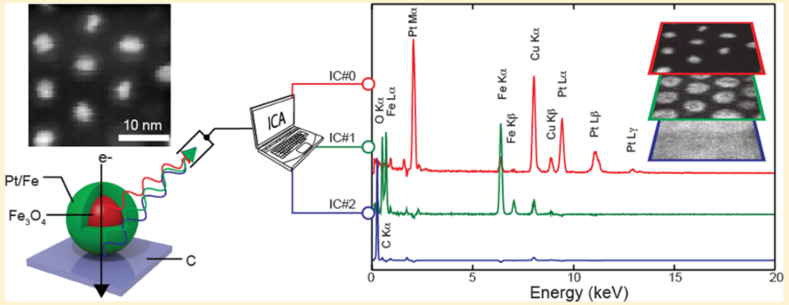

KEYWORDS: *ICA, EDX, TEM, electron microscopy, nanoparticle*

https://github.com/keyoumao/Defect_dP_PaCKage/blob/main/STEM_EDS_demonstration_MSE_FAMU_FSU.ipynb

Montage Demonstration

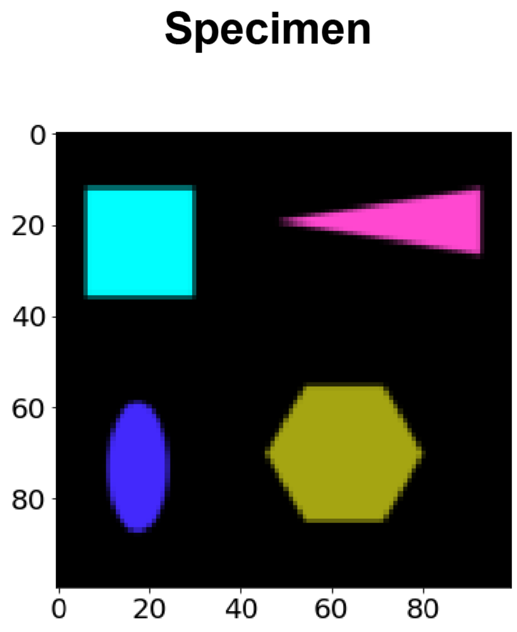

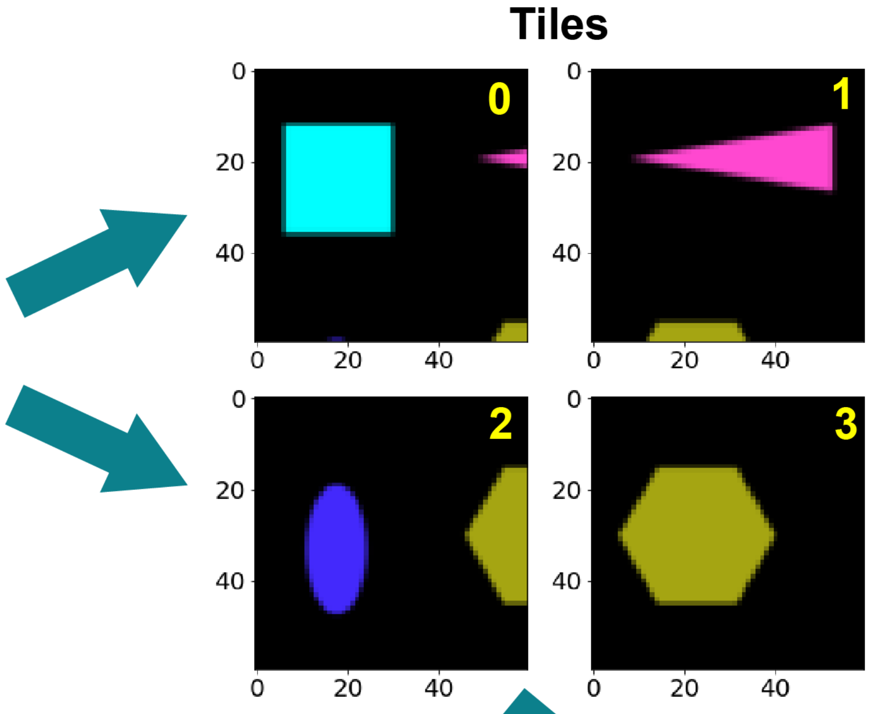

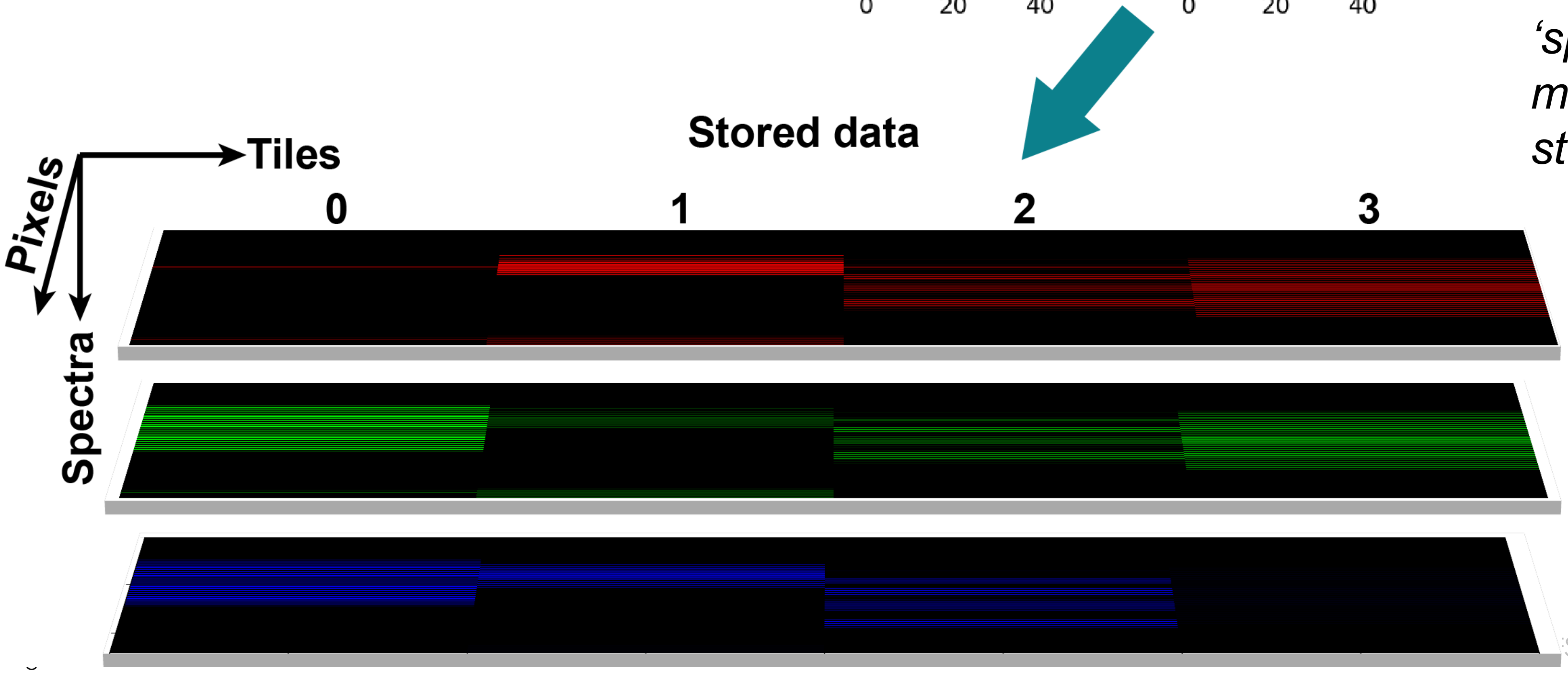

red-green-blue 'spectrum' space, the montage would be stored into a matrix

Large-area EDS on different REBCO tapes

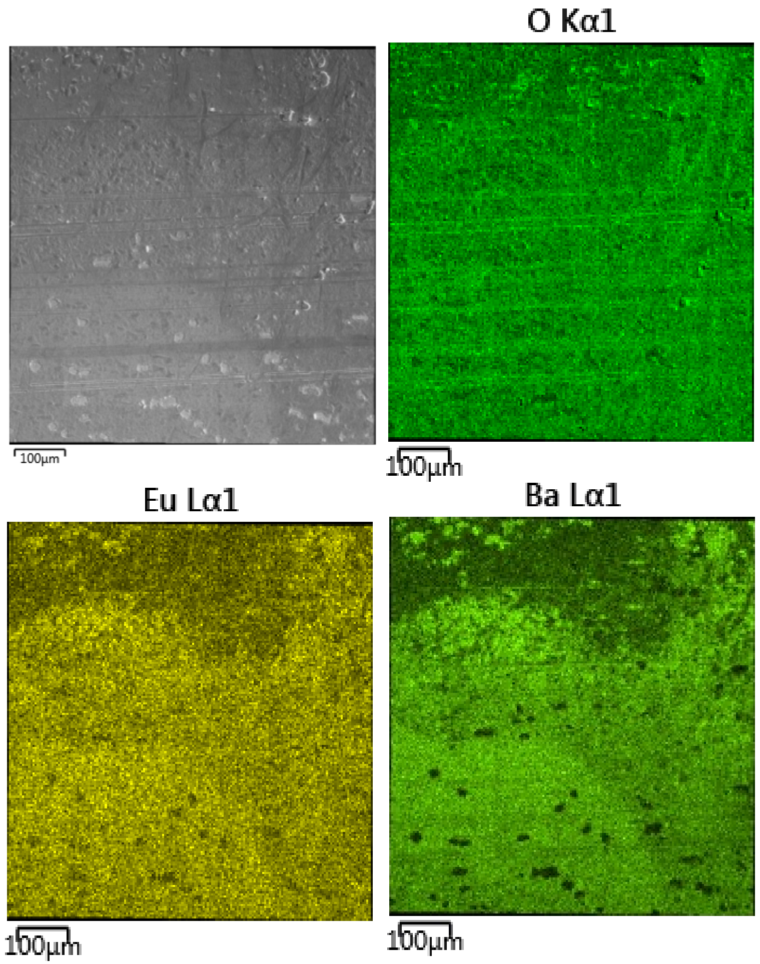

Fujikura

8x11 tiles

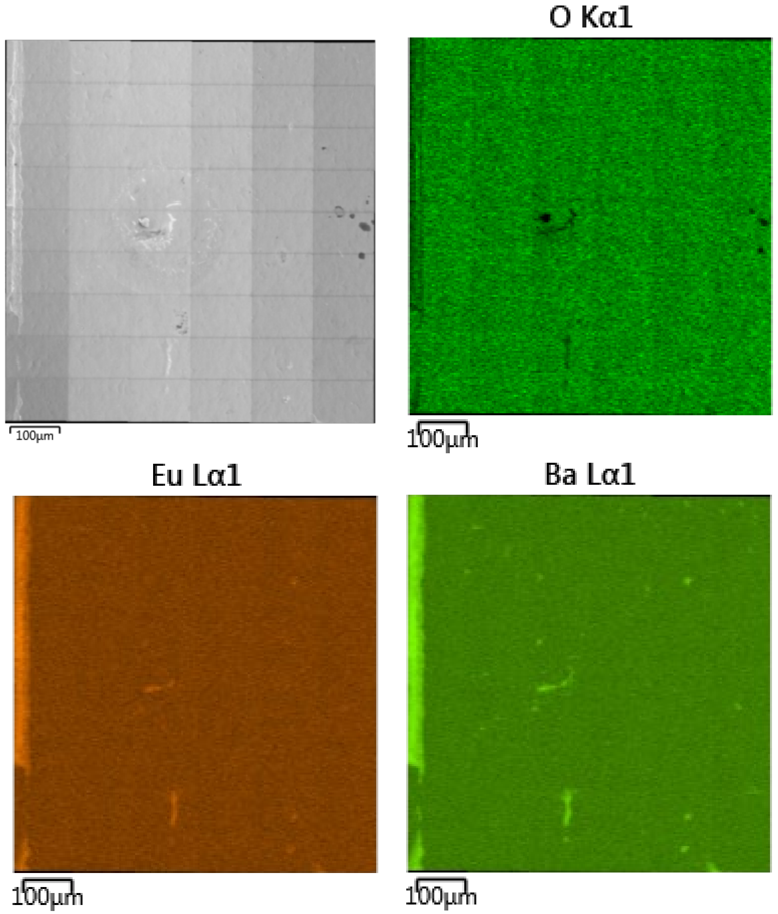

Shanghai

6x9 tiles

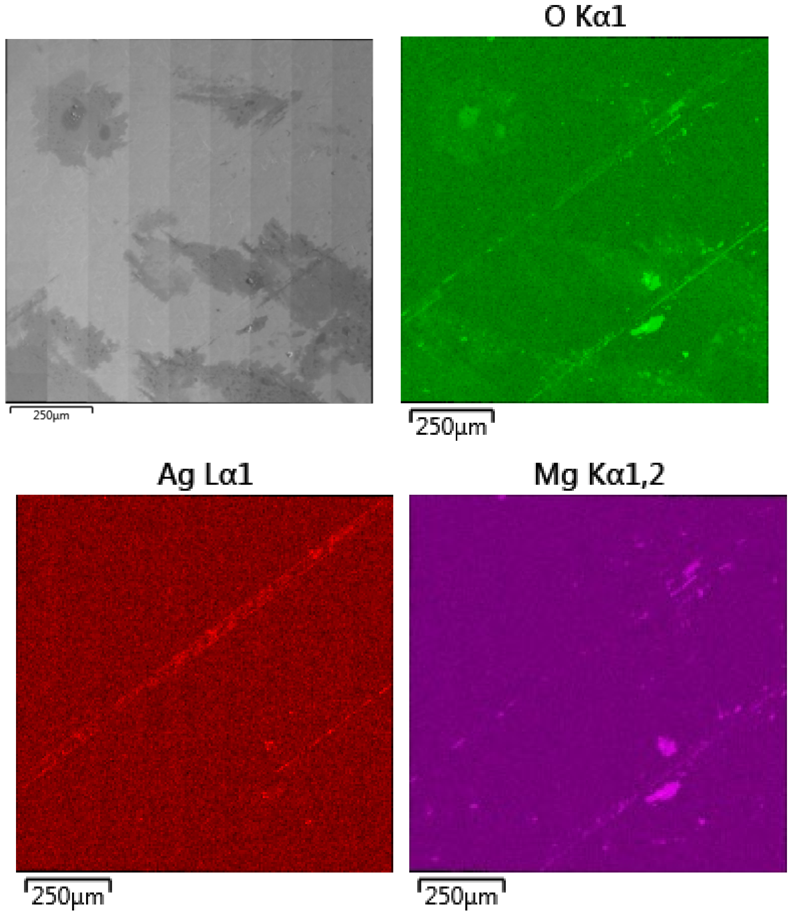

THEVA

9x13 tiles

By Aztec Montage function

Example 2

Large-area XSI maps

Nanoprecipitates / HAADF

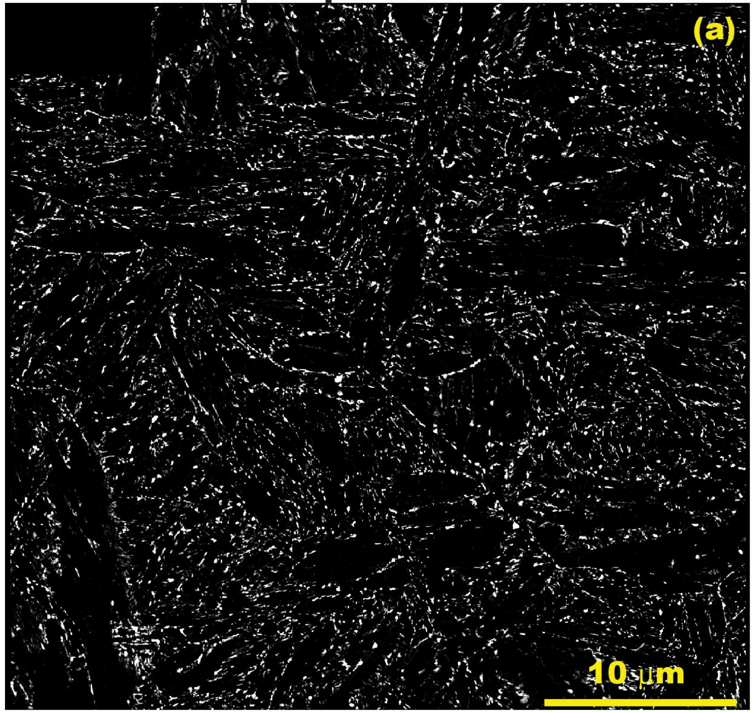

Aluminum / MAADF

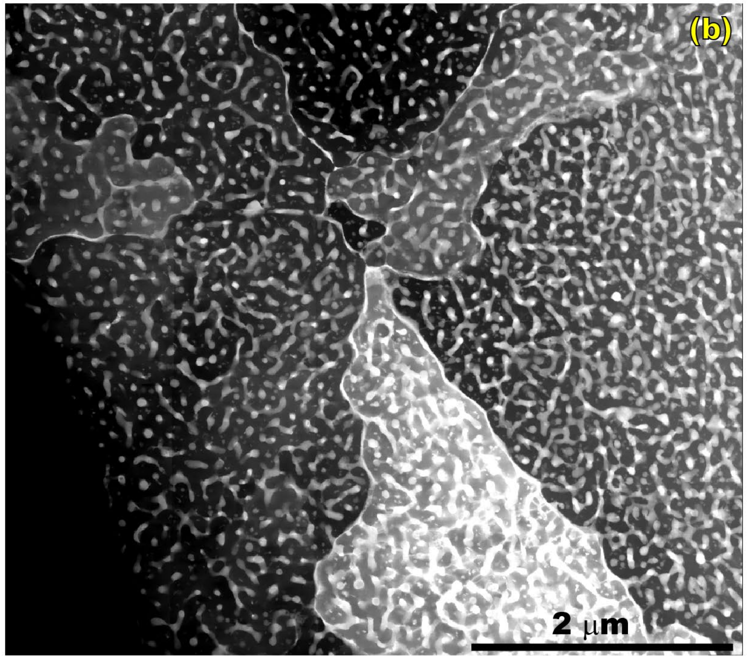

(a) HAADF (high-angle annular dark field) montage of ***10 X 10*** *tiles* **2TB** *from the nanoprecipitate sample. (b) MAADF (medium-angle ADF) montage of* ***5 X 5*** *tiles of the aluminum sample.*

The "nanoprecipitate" sample was an extraction replica from a modified (V-N added) Grade 91 alloy, produced by wire arc additive manufacturing (WAAM), normalized 1100 °C for 30 minutes and tempered at 760 °C for 60 minutes.
Composition was approximately ***Fe-8.4 wt% Cr-0.9Mo-0.3Mn-0.2V-0.1Ni-0.09C-0.04N-0.03O****.*

The aluminum alloy, ***Al-9 wt%Cu-6 wt%Ce*** *nominally, was fabricated via laser powder bed fusion (LPBF) and produced by electropolishing a 3 mm conventional TEM disk.*

10.13139/ORNLNCCS/1806276

Example 2

X-ray maps extracted from the single-tile nanoprecipitate XSI.

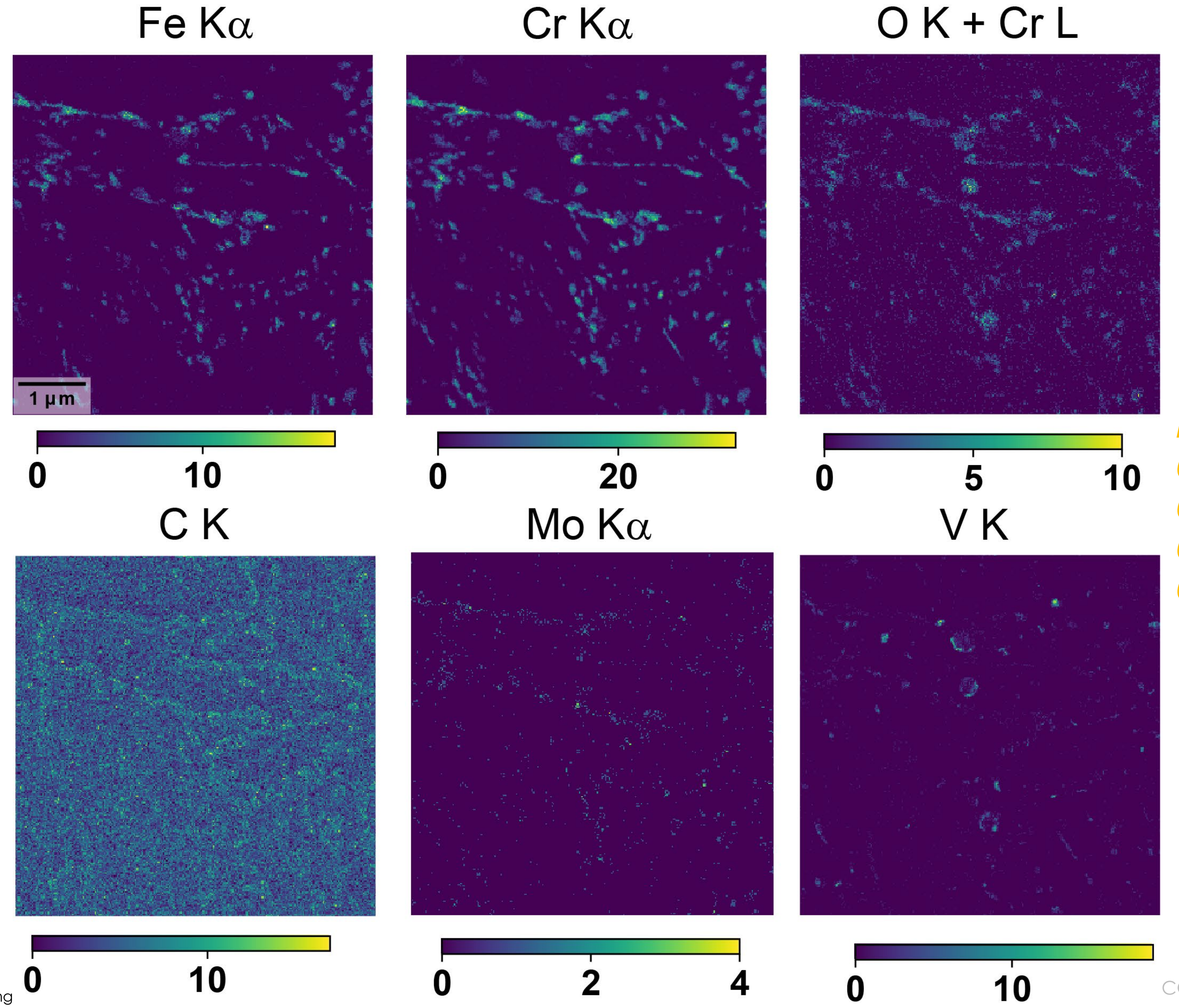

Fe-8.4 wt% Cr-0.9Mo-0.3Mn-0.2V-0.1Ni-0.09C-0.04N-0.03O

10.13139/ORNLNCCS/1806276

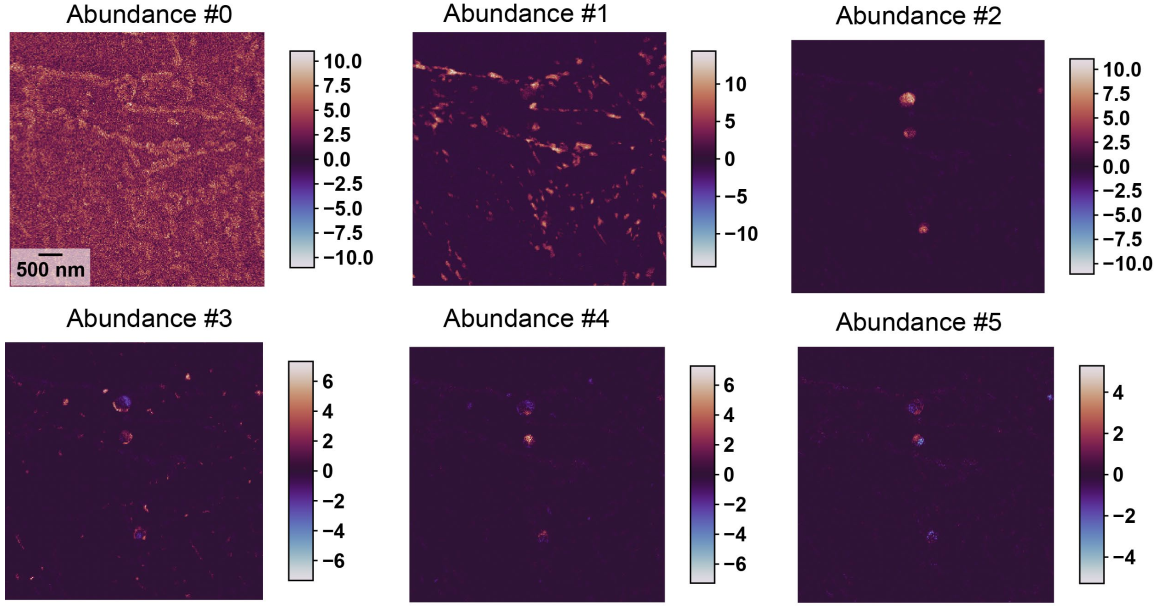

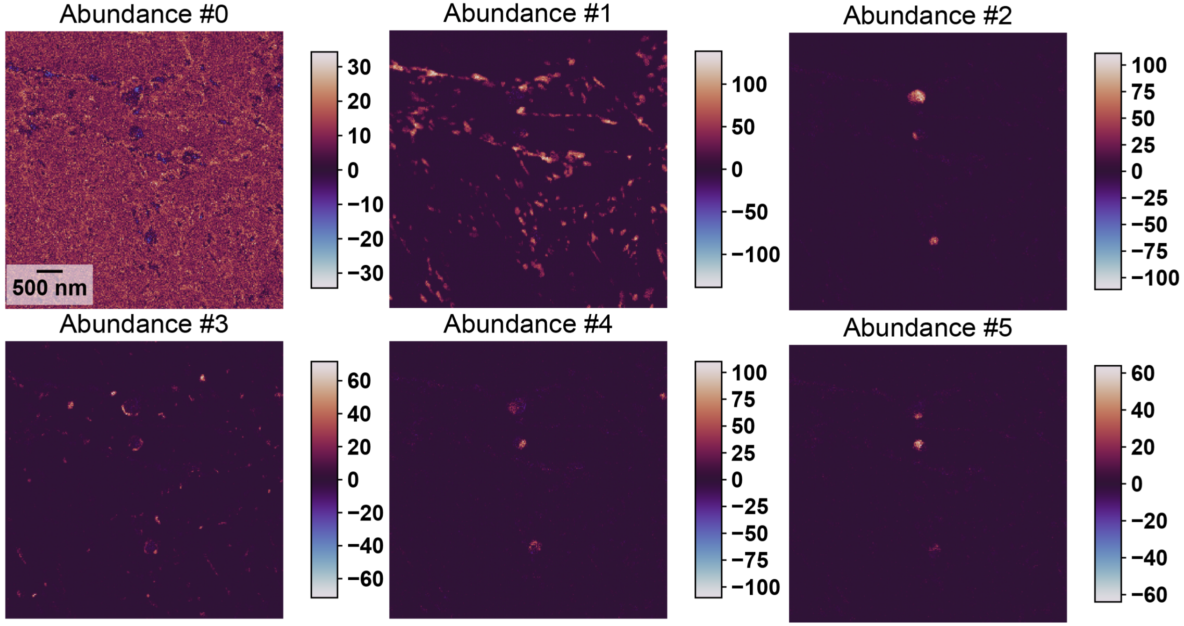

Top row are abundance maps, bottom row spectral endmembers (offset vertically).

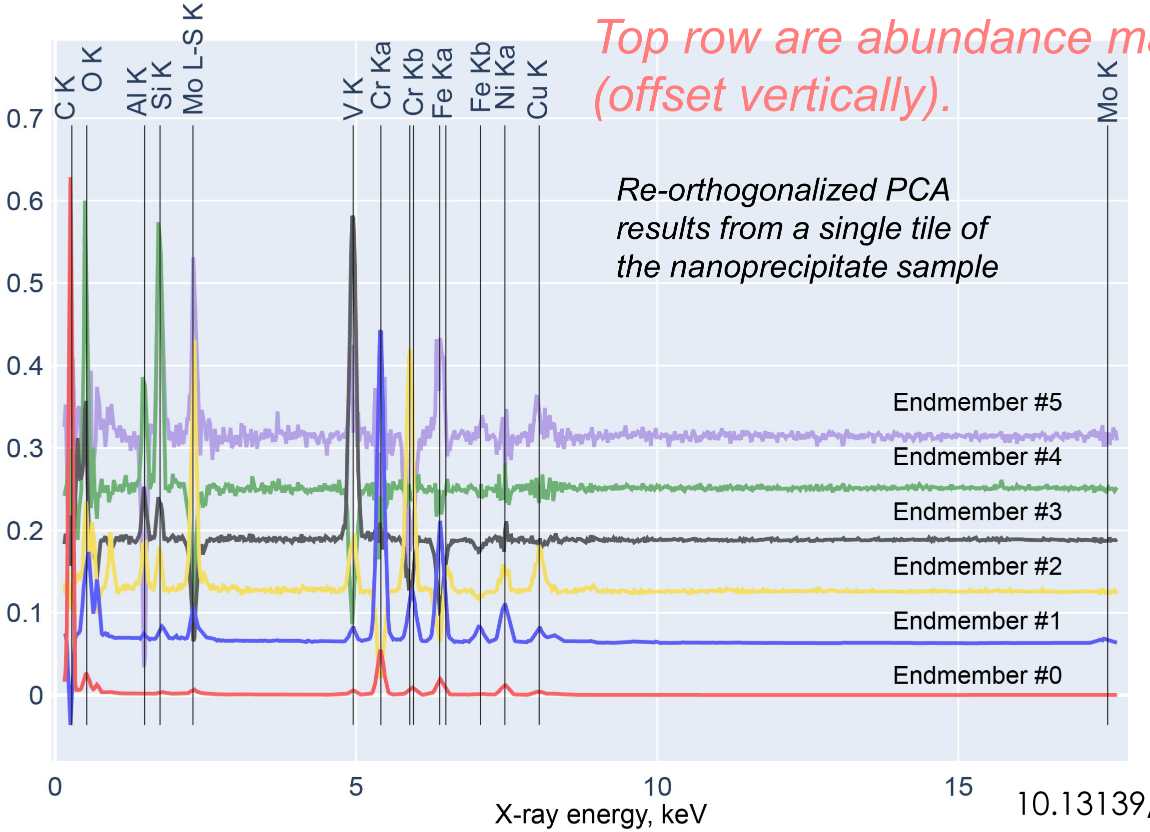

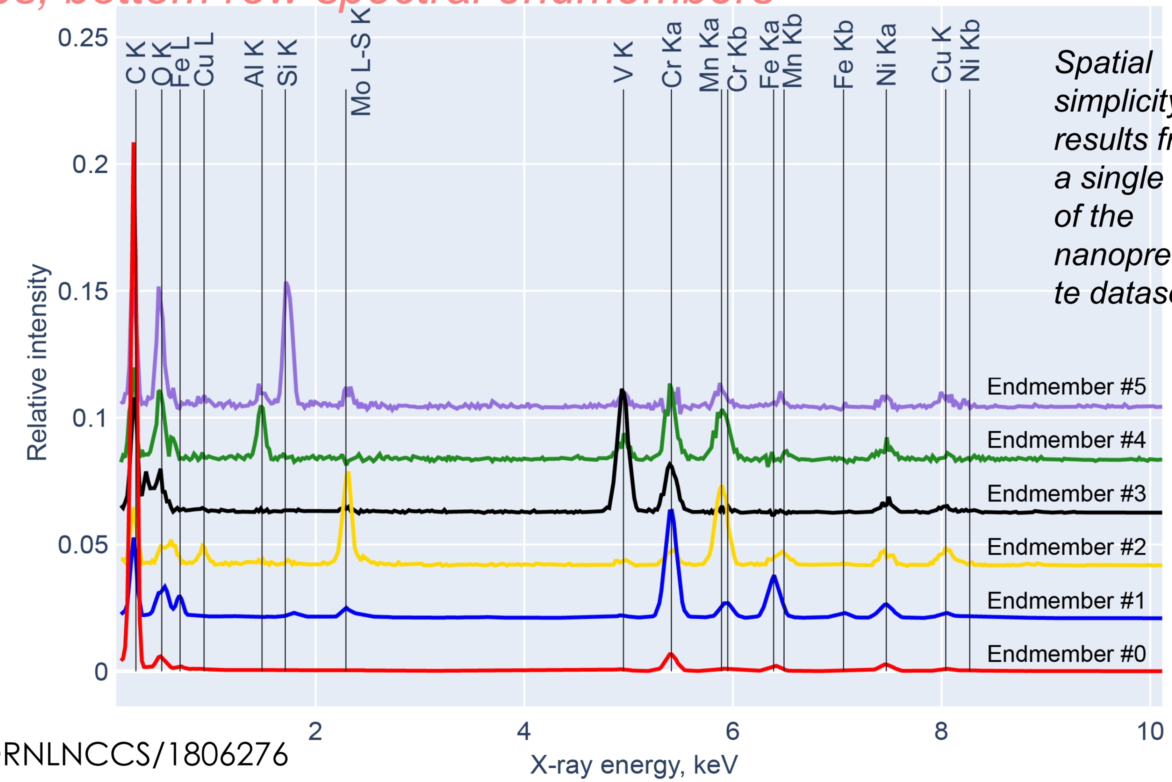

Spatial simplicity results from a single tile of the nanoprecipitate dataset.

10.13139/ORNLNCCS/1806276

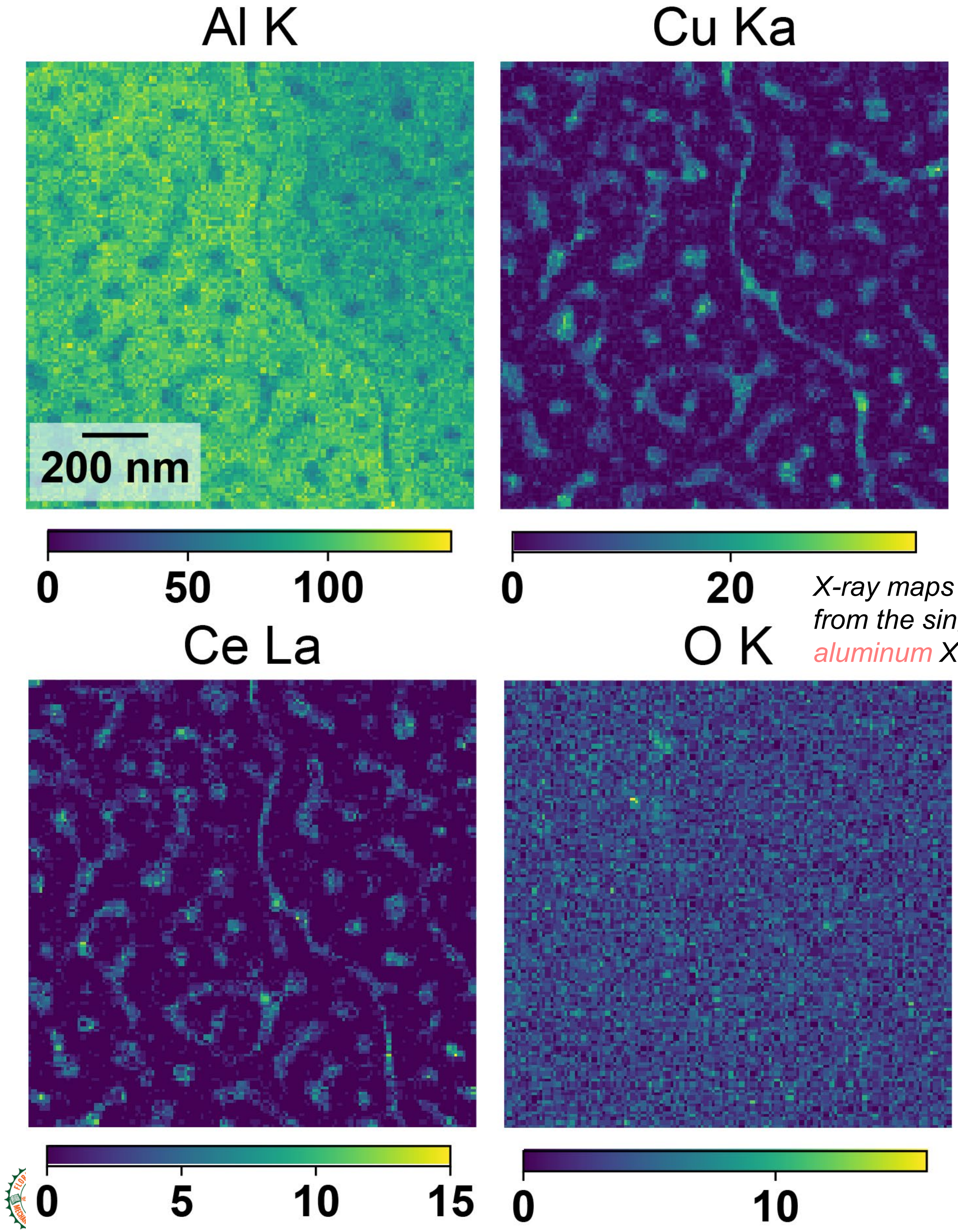

X-ray maps extracted from the single-tile aluminum XSI

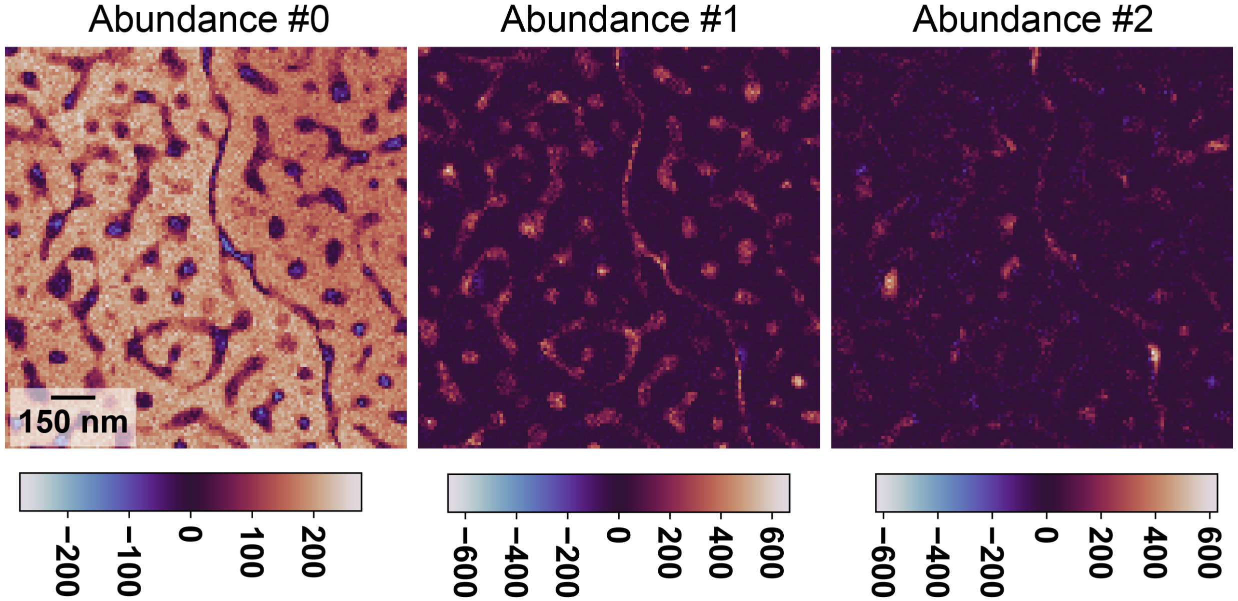

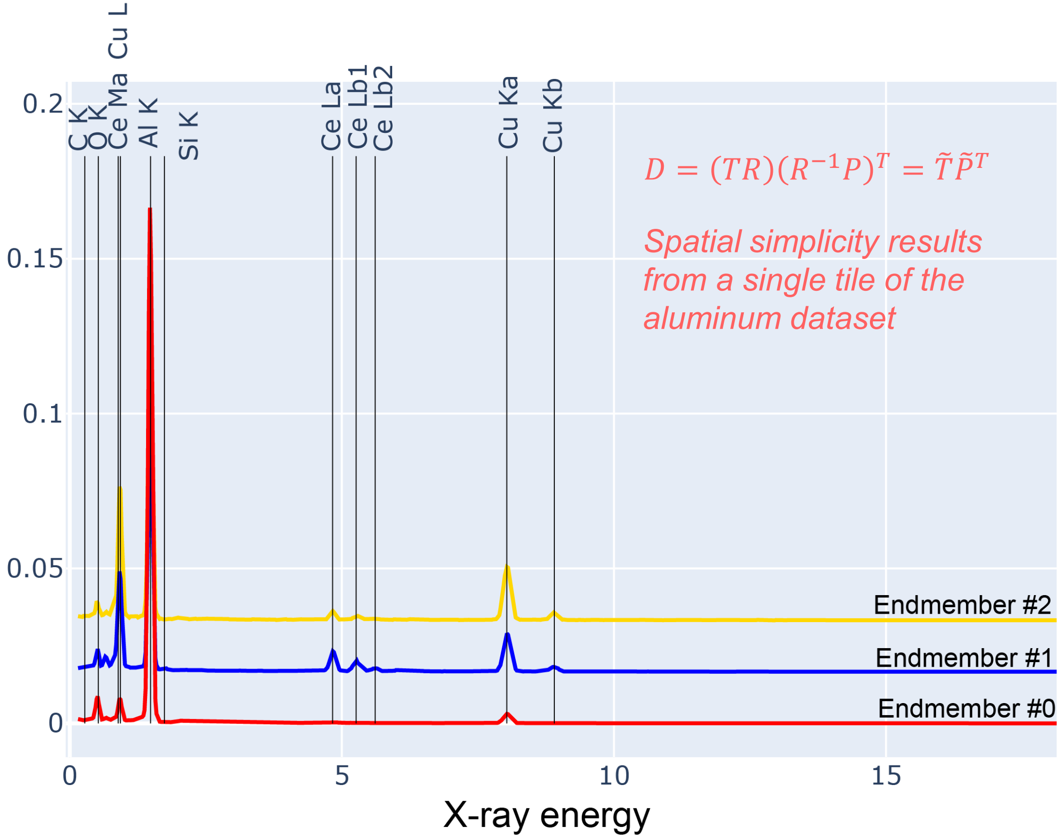

Calculated spatial-simplicity endmembers of ensemble dataset

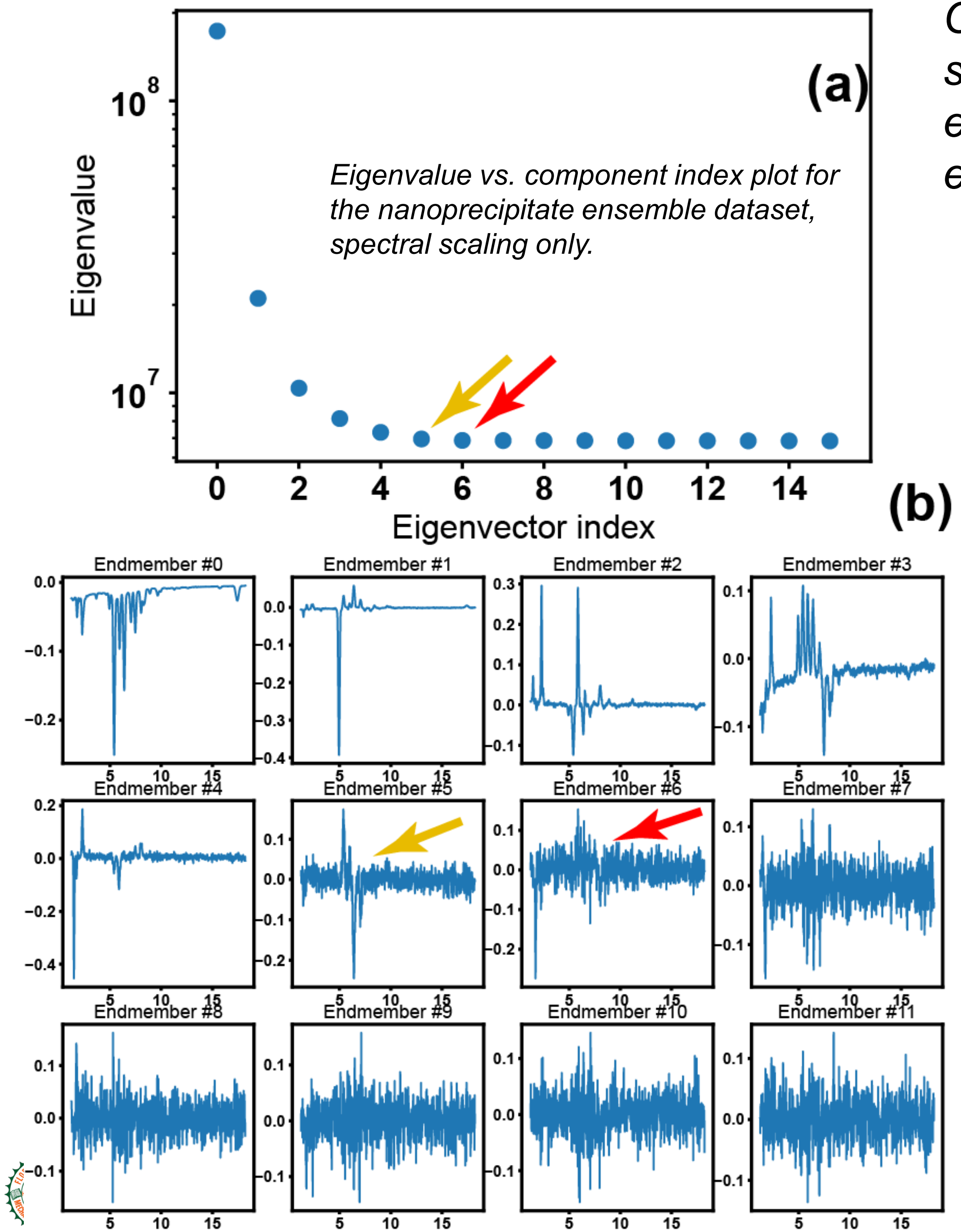

Eigenvalue vs. component index plot for the nanoprecipitate ensemble dataset, spectral scaling only.

The first 12 right singular values (spectral endmembers).

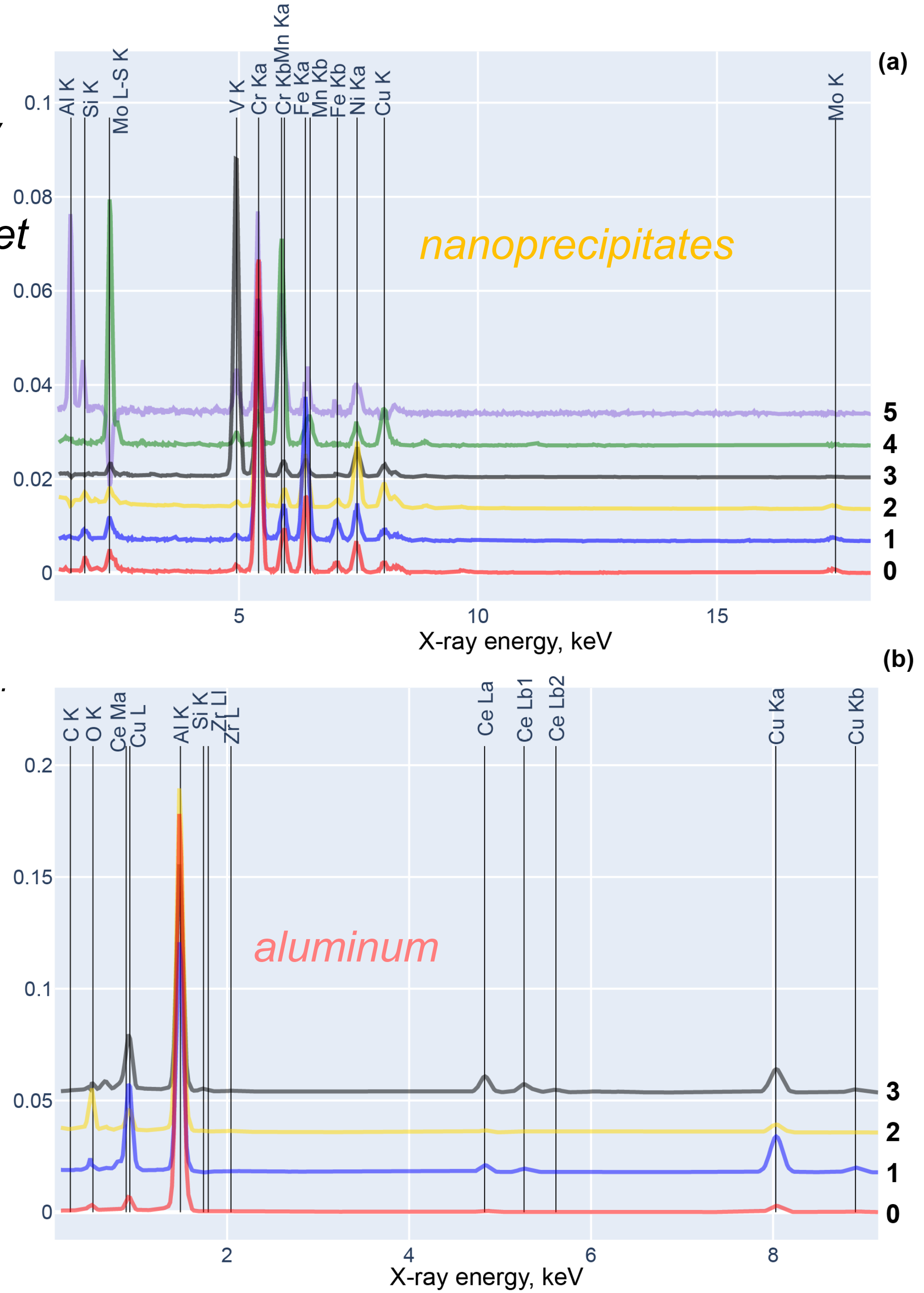

$M_{23}C_6$

Panels #0-#5 are the abundance maps of the endmembers seen in Previous slide the nanoprecipitate dataset.

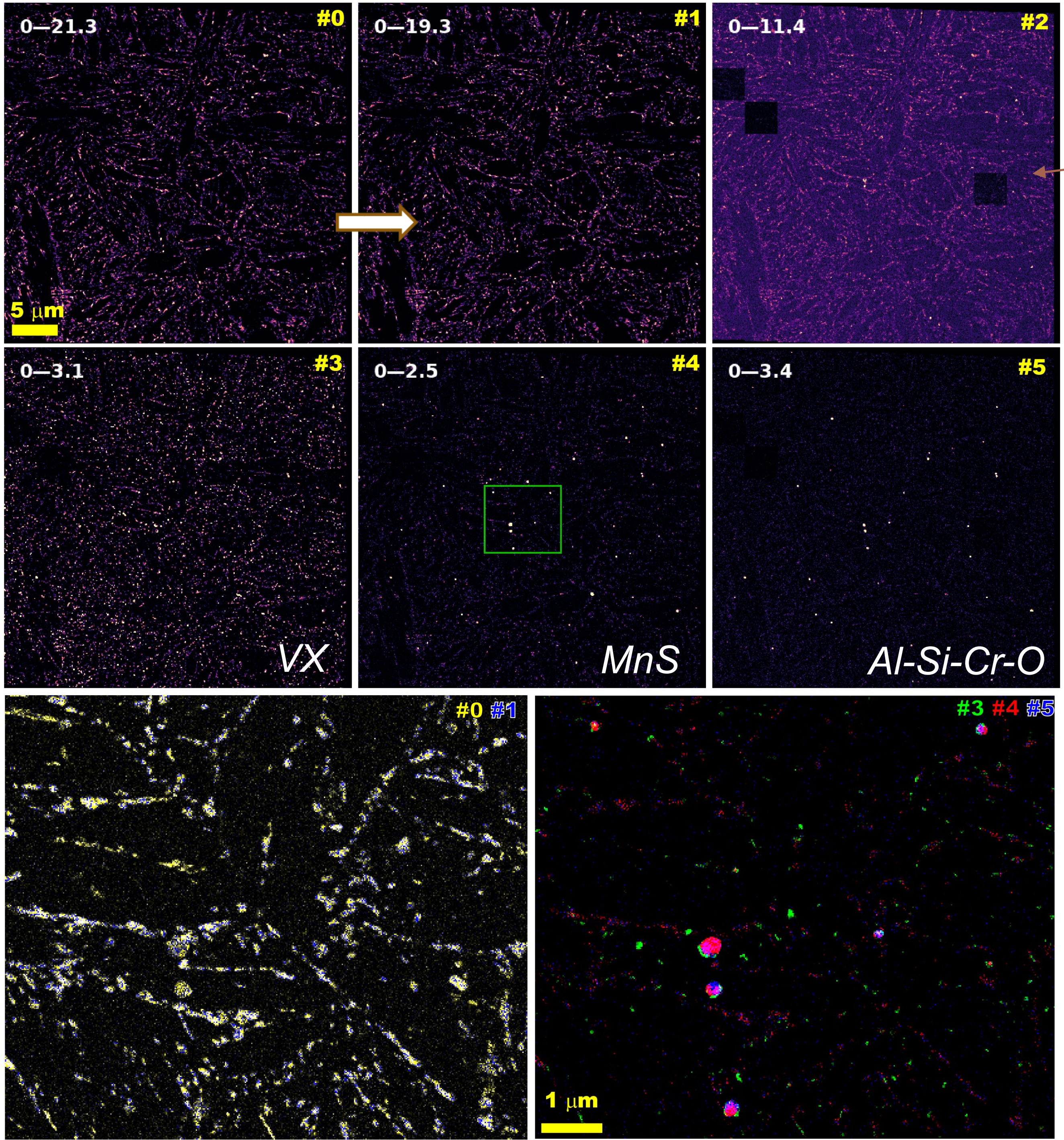

Ni-rich background component.

The bottom row shows false color overlays.

The left overlay shows the two $M_{23}C_6$ components as yellow and blue;

the right overlay shows the VX, MnS, and Al-Si-Cr components.

Matrix

Panels #0, #1, #2, and #3 are the abundance maps of the spatial-simplicity endmembers from the aluminum dataset

aluminum oxide

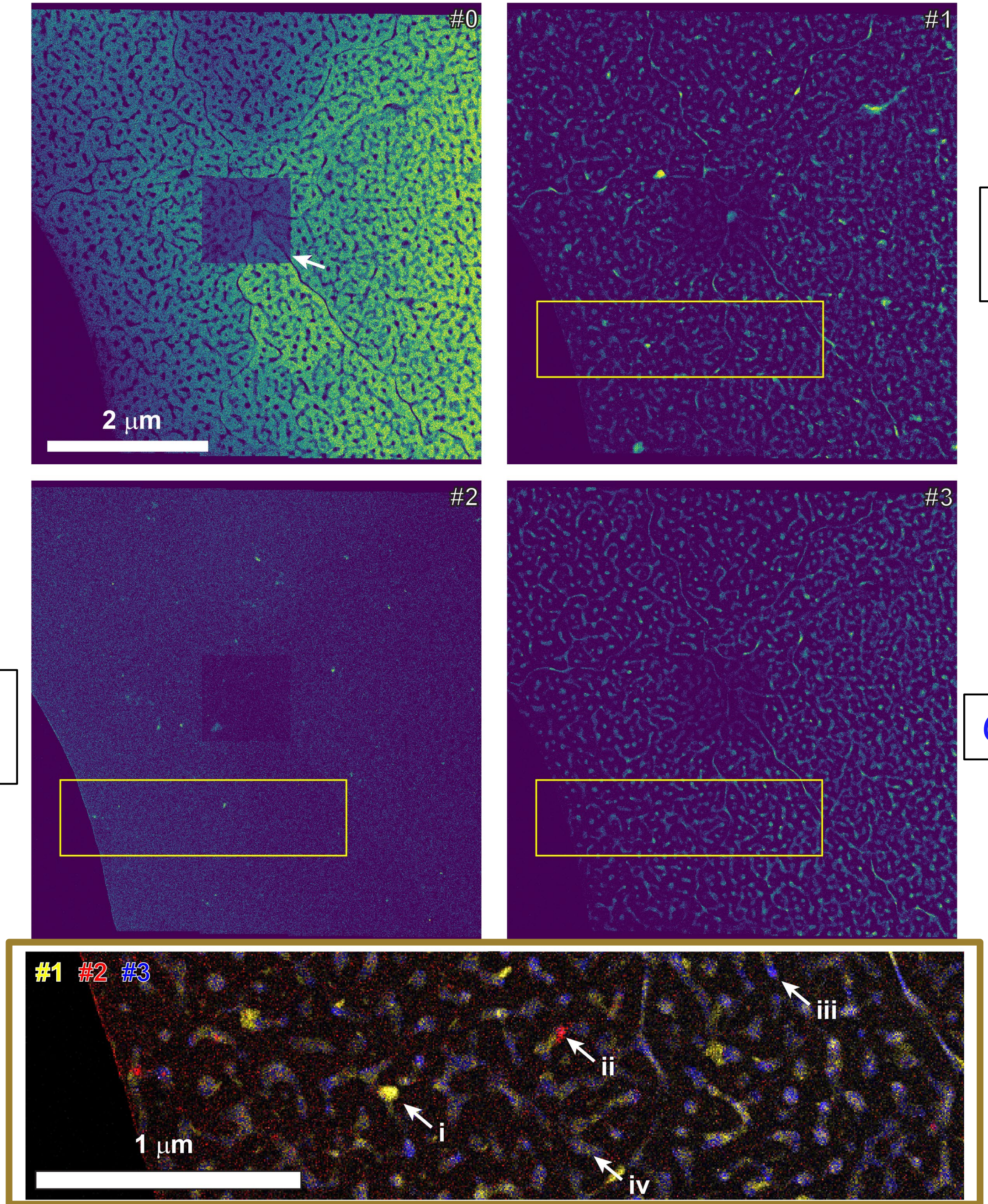

Cu-rich, Ce-poor

Cu-Ce

The arrow denotes a tile with low X-ray counts

References

Hyperspy

http://hyperspy.org/hyperspy-doc/current/index.html

Atomai

https://atomai.readthedocs.io/en/latest/

Pycroscopy

https://pycroscopy.github.io/pycroscopy/ecosystem.html

Py4DSTEM

https://py4dstem.readthedocs.io/en/latest/index.html

OpenCV

https://docs.opencv.org/4.x/d9/df8/tutorial_root.html

Code for EDS

https://github.com/keyoumao/ML_FUEL_CM_COMMSMAT

Today's materials

https://github.com/keyoumao/Defect_dP_PaCKage

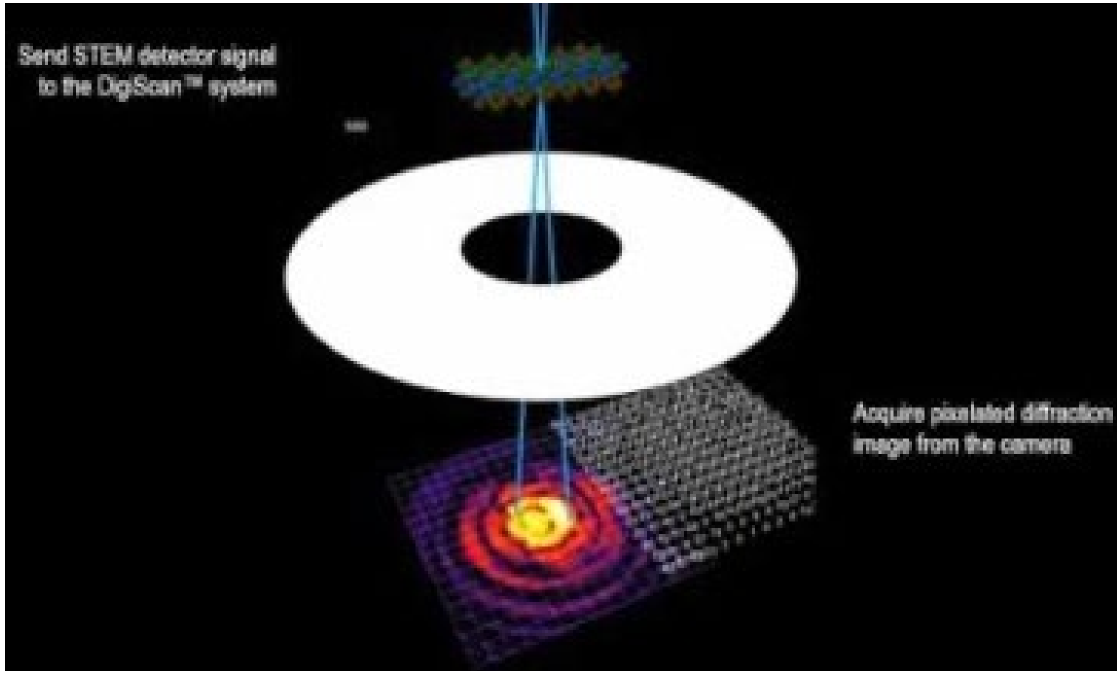

Contributions

- Successful characterization on materials in extreme conditions can be accomplished with the aid of modern electron microscopy to understand the **processing-structure-property** relationship.

- A Machine Learning (ML)-enhanced approach has been implemented for X-ray spectrum image mapping (XSI), where this method can facilitate the current data acquisition and analysis cycle by at least 1 magnitude of order.

- This ML enhanced approach can be coupled with **deep learning** and other **automapping** software or open-access platform to identify nanoclusters with increased confidence and accuracy.

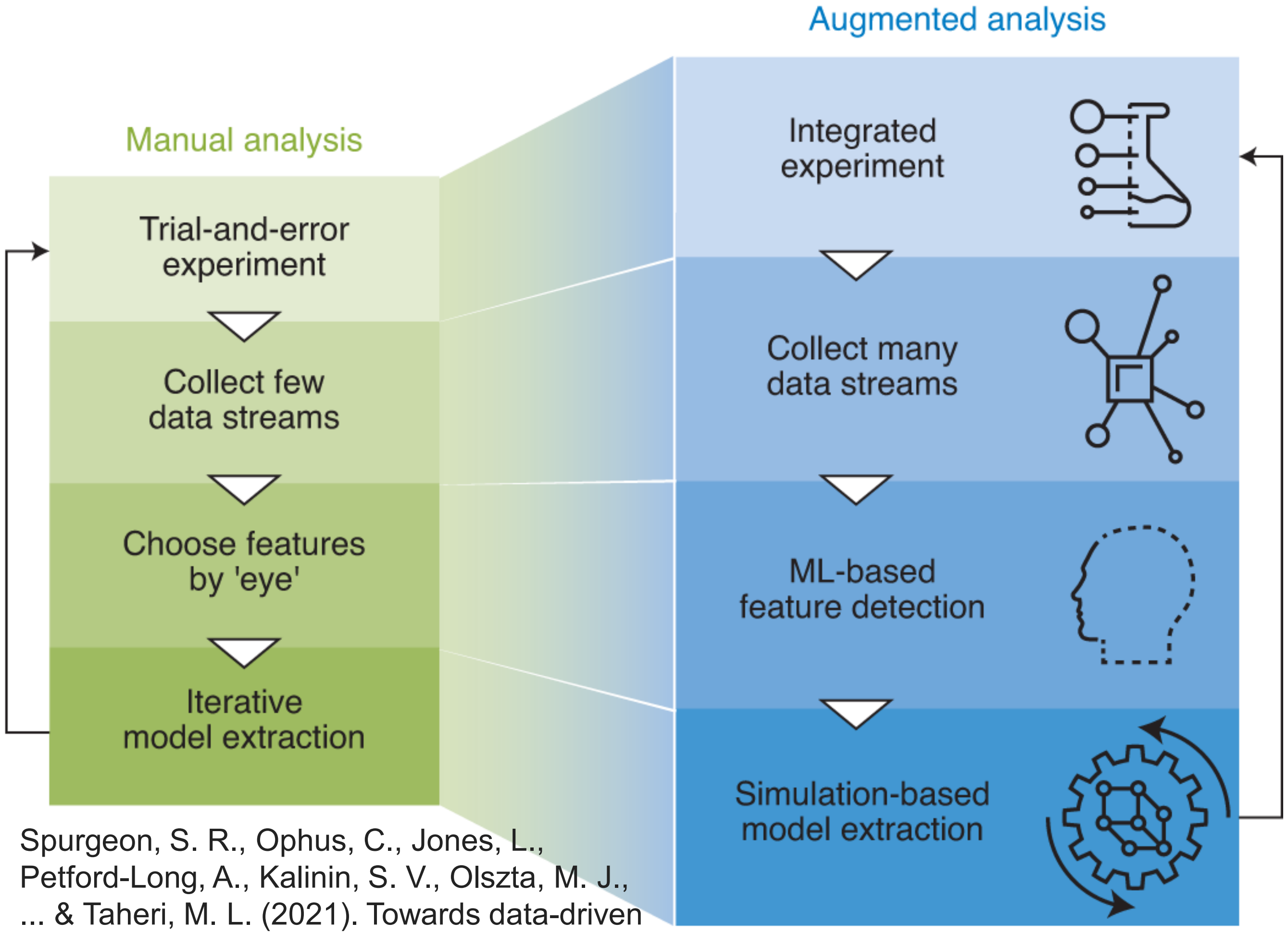

Spurgeon, S. R., Ophus, C., Jones, L., Petford-Long, A., Kalinin, S. V., Olszta, M. J., ... & Taheri, M. L. (2021). Towards data-driven next-generation transmission electron microscopy. *Nature materials*, *20*(3), 274-279.

NATIONAL HIGH MAGNETIC FIELD LABORATORY

Sub-Ångström Resolution, World-Leading Analytical Electron Microscopy Facility: Analysis at the Atomic Level with Liquid-Cell

Aerial view of National MagLab

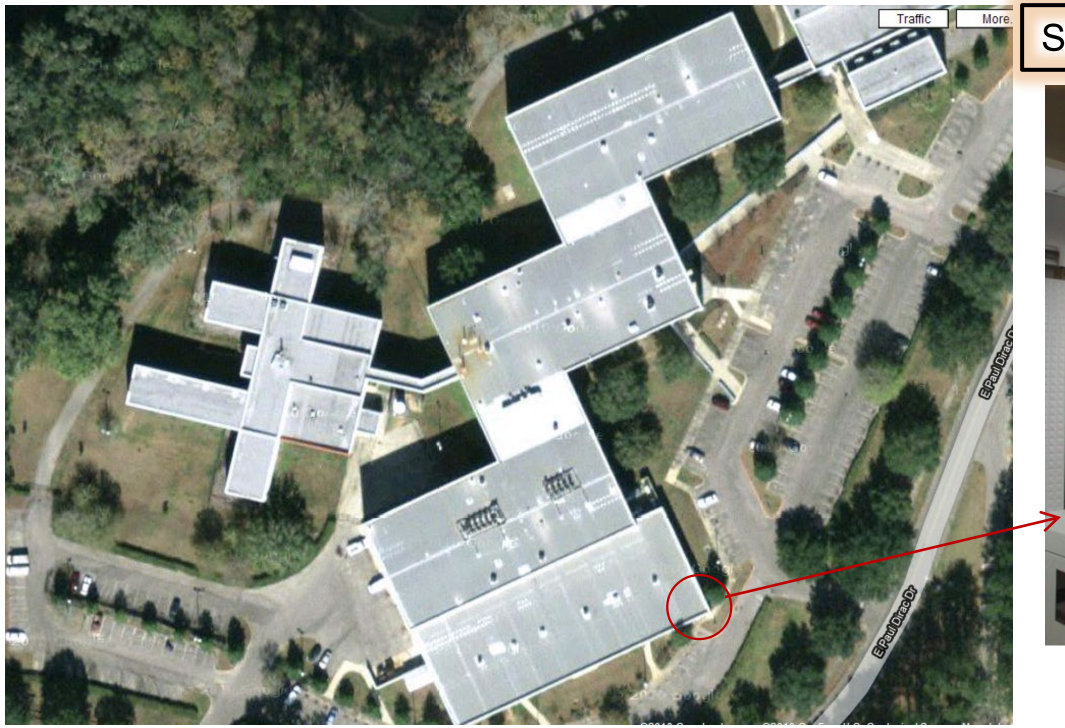

State-of-the-art Transmission Electron Microscope

Thermo Fisher Scientific Dual Beam Focused Ion Beam/Field Emission Scanning Electron Microscope

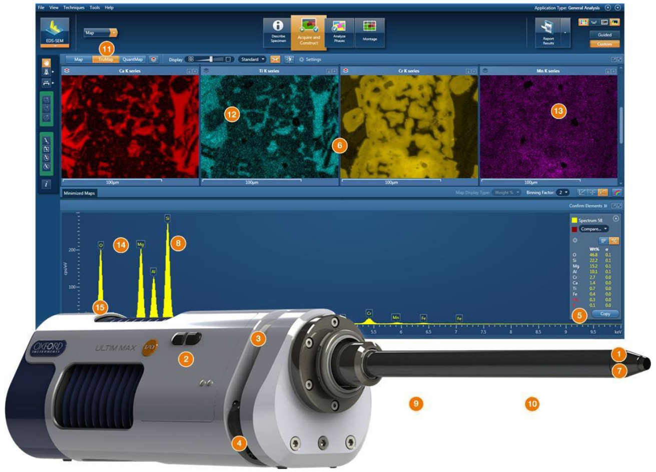

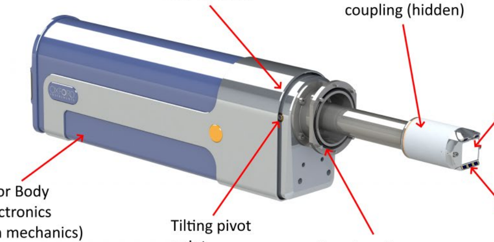

Helios G4 UC with Oxford detect

- •FIB: AutoSlice software allows for highest quality, fully automated acquisition of multimodal **3D datasets**.
- •EBSD/EDS: **Montage, large-area EDS automated mapping from Oxford Aztec upgrade.**
- **•New workstation for the automated analysis on spectrum images and 3D reconstruction.**

amazon Rekognition

- •STEM: Two-segment solid-state STEM detector for high-resolution bright and dark field imaging of FIB-prepared cross sections and critical dimension measurements. e.g. **dislocation imaging, phase contrast** mapping.

This state-of-the-art transmission electron microscope is funded by Florida State University Research Foundation and supported by National High Magnetic Field Laboratory (funded by National Science Foundation) and the State of Florida.

To gain access, we welcome interested parties to contact us:

Sam Mao, Ph.D.
Department of Industrial and Manufacturing
Florida A&M University-Florida State University
College of Engineering

2525 Pottsdamer St.,
Tallahassee, FL 32310-6046
E-mail: kmao@eng.famu.fsu.edu

Yan Xin, Ph.D.
National Magnetic Field Laboratory
Florida State University

1800 E. Paul Dirac Drive,
Tallahassee, FL 32310
E-mail: xin@magnet.fsu.edu

New 4D STEM detector will be online!